International Journal of Heat and Mass Transfer 146 (2020) 118864

Contents lists available at ScienceDirect

International Journal of Heat and Mass Transfer

journal homepage: www.elsevier.com/locate/ijhmt

Review of channel flow boiling enhancement by surface modification, and instability suppression schemes

Gangtao Liang [a], Issam Mudawar [b,*]

[a] Key Laboratory of Ocean Energy Utilization and Energy Conservation of Ministry of Education, School of Energy and Power Engineering, Dalian University of Technology, Dalian 116024, China
[b] Purdue University Boiling and Two-Phase Flow Laboratory (PU-BTPFL), School of Mechanical Engineering, 585 Purdue Mall, West Lafayette, IN 47907, USA

ARTICLE INFO

Article history:
Received 11 May 2019
Received in revised form 7 October 2019
Accepted 8 October 2019
Available online 25 October 2019

Keywords:
Flow boiling
Enhancement
Surface modification
Heat transfer coefficient
Critical heat flux (CHF)
Pressure drop

ABSTRACT

This article provides a comprehensive review of published literature concerning enhancement of channel flow boiling heat transfer by surface modification. Addressed are macro, micro, nano, and hybrid multi-scale methodologies. While the vast majority of published schemes have shown favorable heat transfer performance, evidenced by earlier onset of boiling, improved flow boiling heat transfer coefficient, and ameliorated critical heat flux (CHF), increased pressure drop is a serious concern shared by most. Nanoscale enhancement remains controversial, given that, unlike macroscale and microscale enhancement features, nanostructure topographies are prone to severe degradation after prolonged boiling. Multiscale enhancement, combining macro, micro, and nano features as well as favorable coolant flow control, is shown highly effective at tackling very high heat flux situations. Also included in this review is discussion of effective means for mitigating flow instabilities. It is concluded that the most serious obstacle to adopting surface modification techniques is absence of generalized predictive tools or robust computational models for different channel shapes, sizes, and enhancement configurations, and different fluids and operating conditions, such as tools presently available for two-phase flow and heat transfer in conventional micro-channel heat sinks.

Contents

* Corresponding author.
E-mail address: mudawar@ecn.purdue.edu (I. Mudawar).
URL: https://engineering.purdue.edu/BTPFL (I. Mudawar).

https://doi.org/10.1016/j.ijheatmasstransfer.2019.118864
0017-9310/

Nomenclature

Bo	Bond number
Co	confinement number
D_h	hydraulic diameter
d_p	particle diameter
G	mass velocity
g	gravitational acceleration
h	heat transfer coefficient
l_c	capillary length
p	pressure
Δp	pressure drop
q''	surface heat flux
T	temperature
t	time
ΔT_{sat}	surface superheat, T_w - T_{sat}
ΔT_{sub}	subcooling, T_{sat} - T_{in}

Greek symbols

ε	ratio of ε_h to $\varepsilon_{\Delta p}$
ε_h	heat transfer enhancement factor
$\varepsilon_{\Delta p}$	pressure drop penalty factor
ρ	density
σ	surface tension

Subscripts

f	liquid
g	vapor
in	inlet
out	outlet
pt	plain tube
sat	saturation
st	structured (surface enhanced) tube
sub	subcooling
w	surface

1. Introduction

1.1. Modern high heat flux cooling applications

During the past three decades, aggressive miniaturization of electronic components has spurred an urgent need for more effective thermal management solutions that could maintain device temperatures safely below specific material and performance limits. This trend began mostly in the early 1980s, when rapid escalation in heat dissipation prompted a transition from reliance on fan-cooled heat sink attachments to a variety of liquid cooling schemes. Initially, only single-phase liquid cooling solutions were sought. But, in the late 1980s, heat dissipation from supercomputers chips approached the 100 W/cm^2 threshold, exceeding the capabilities of most single-phase liquid cooling solutions [1]. This rapid escalation in heat dissipation made inevitable the need to transition from single-phase to two-phase cooling. Key to this transition is ability of two-phase solutions to capitalize upon the coolant's both sensible and latent heat rather than sensible heat alone.

Today, high heat flux cooling is no longer confined to computer electronics. Heat dissipation challenges are prevalent in a broad variety of applications, including x-ray medical devices, hybrid vehicle power electronics, heat exchangers for hydrogen storage, fusion reactor blankets, particle accelerator targets, magnetohydrodynamic (MHD) electrode walls, rocket nozzles, aircraft, satellite and spacecraft avionics, laser and microwave directed energy weapons, advanced radar, turbine blades, and air-to-fuel heat exchangers in high-Mach aircraft [2]. Rapid developments in these and other applications have now shifted interest to cooling solutions that could surpass a new 1000 W/cm^2 threshold [3].

A key design objective in developing thermal solutions for the applications just mentioned is to maintain operation in the nucleate boiling regime in order to capitalize on the high heat transfer coefficients attainable within this regime and therefore maintain low device temperatures. Another objective is to identify coolant operating conditions that would maintain critical heat flux (CHF) limit safely above the device heat flux, as shown in Fig. 1. CHF represents the most important safety limit for any heat-flux-controlled two-phase cooling system, as exceeding this limit could

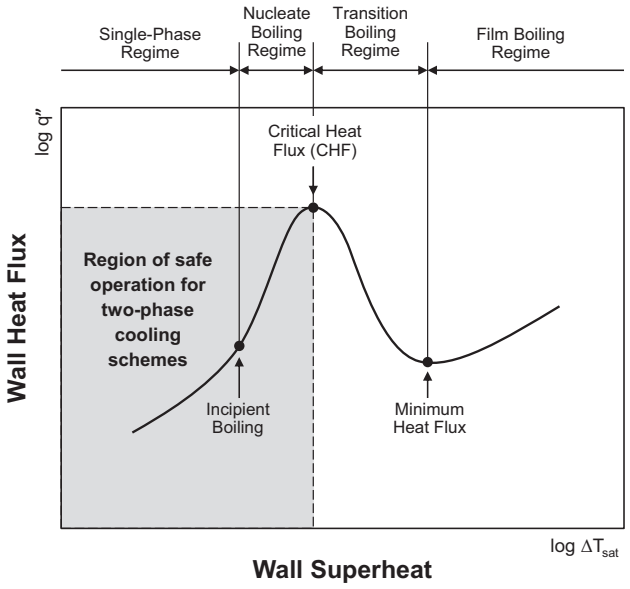

Fig. 1. Region of safe operation in boiling curve for two-phase cooling schemes.

trigger rapid and unsteady transition from highly efficient nucleate boiling to heat transfer deficient film boiling, which is accompanied by sharp escalation in device temperature, culminating in serious device damage.

1.2. Two-phase cooling solutions and potential problems

Responding to the trend of increasing heat dissipation, a variety of thermal management solutions have been proposed [2,4]. Such solutions have been a primary focus for a series of experimental and theoretical studies at the Purdue University Boiling and Two-Phase Flow Laboratory (PU-BTPFL) spanning over three decades. They include passive (pump-free) cooling schemes, including capillary-driven devices (heat pipes, capillary pumped loops, and loop heat pipes) [5] and pool boiling thermosyphons [6], techniques that are intended to tackle relatively moderate heat fluxes. But most solutions investigated at PU-BTPFL concern high heat fluxes where a liquid pump is required to boost convective cooling rate. Examples include two-phase schemes utilizing falling films [7], macro-channel flow boiling [8–12], mini/micro-channel flow boiling [13–17], jet-impingement [18], and spray [19–22], as well as hybrid cooling schemes combining the merits of mini/micro-channel flow boiling and jet impingement [23].

Aside from pointing out well-established merits of two-phase cooling schemes, it is equally important to mention their shortcomings. As indicated in [24], they include *temperature overshoot* that accompanies nucleate boiling inception in highly wetting dielectric fluids, including FC-72, FC-87, HFE-7100, and various refrigerants, associated with which is potentially damaging thermal cycling during power transients. The second is *bubble layer growth* along multi-device cooling modules, which could compromise cooling of downstream devices by the vapor wake produced from upstream devices. A related problem is *high pressure drop*, brought about by vapor formation, coalescence, and growth along the cooling module. Another concern is *inability to achieve sufficiently high CHF*, especially when using dielectric fluids, which possess relatively poor thermal transport properties, especially latent heat of vaporization.

Another concern with two-phase cooling systems is prevalence of a variety of *flow instabilities*. For example, in micro-channel heat sinks widely recommended for high heat flux situations, bubble growth along parallel small diameter channels has been shown to induce appreciable flow fluctuations [25], and, in extreme cases, flow reversal, partial dry out, and pre-mature CHF [13].

Studies have shown that combining merits of phase change and high coolant flow rate still falls short of tackling the high heat fluxes presently encountered or projected [26]. The need to both improve nucleate boiling heat transfer coefficient (in order to lower surface temperature) and increase CHF is a primary reason for adopting surface enhancement techniques in two-phase cooling applications. In fact, recent research efforts have focused mostly on further amelioration of cooling performance, especially CHF, through reliance on surface modification enhancement. The present article is dedicated entirely to surface modification strategies intended for channel flow boiling.

1.3. Demarcation of channel dimensions

Before addressing suitability of different surface modification schemes to channel flow boiling, it is vital to distinguish cooling configurations based on hydraulic diameter of flow passages, given the vast differences in flow boiling patterns encountered in small (micro) versus macro-channels.

Investigators have adopted a variety of criteria to distinguish channel size categories. Kew and Cornwell [27] recommended demarcating macro- and micro-channels based on magnitude of confinement number, *Co*, defines as

$$Co = \left[\frac{\sigma}{g\left(\rho_f - \rho_g\right)D_h^2}\right]^{1/2}, \tag{1}$$

where σ, g, ρ_f, ρ_g, and D_h are, respectively, surface tension, gravitational acceleration, liquid density, vapor density, and channel hydraulic diameter.

Ong and Thome [28] recommended demarcation into three size ranges: micro-channel for $Co > 1$, macro-channel for $Co = 0.3–0.4$, and in-between transitional range corresponding to $0.3–0.4 \le Co \le 1.0$. Mehendale et al. [29] provided a much simpler classification using hydraulic diameter alone: micro-channel for 1–100 μm, mini-channel for 100–1000 μm, and macro-channel above 1000 μm.

Cheng et al. [30] recommended an alternative classification based on Bond number, *Bo*, defined in terms of ratio of hydraulic diameter to capillary length (l_c),

$$Bo = \left(\frac{D_h}{l_c}\right)^2 = \frac{g\left(\rho_f - \rho_g\right)D_h^2}{\sigma}. \tag{2}$$

Unlike the classifications of Kew and Cornwell and Ong and Thome, the *Bo* classification also accounts for gravitational effects: micro-channel for $Bo < 0.05$, where gravitational effects are negligible, mini-channel for $0.05 < Bo < 3$, where surface tension effects are dominant and gravitational effects weak, and macro-channel for $Bo > 3$, where surface tension is much weaker than gravitational force.

1.4. Heat transfer enhancement techniques

Methodologies that have been proposed to improve heat transfer fall into one of two categories [31]: *active* or *passive*. The active techniques require external power, including use of a mechanical pump, mechanical mixing, surface and/or liquid rotation and vibration, suction or injection, and addition of external electrostatic or magnetic field. Aside from using a pump to supply coolant, most other active techniques are both costly and difficult to implement in compact cooling situations, such as those intended for electronic devices. On the other hand, passive heat transfer enhancement is realized by altering fluid properties and/or heat transfer surface.

The latter involves modifying surface shape and/or roughness, or attaching fins to increase surface area and turbulence, and ameliorate bubble nucleation.

This study is focused on enhancement of channel flow boiling using only surface modification techniques. One of the motivations here is the need to improve heat transfer performance of two-phase thermal management systems in space vehicles. Studies have shown great reductions in CHF in the absence of gravity, which could endanger safety of the entire thermal management system [32–35]. Two methods to ameliorating CHF are (1) relying on high coolant flow velocity, which serves to detach vapor bubbles from the surface and combat formation of an insulating vapor layer, and (2) incorporating effective surface enhancement schemes.

1.5. Prior reviews on heat transfer enhancement using surface modification

Enhancement of flow boiling heat transfer by surface modification has been the subject of several review articles, some addressing enhancement of pool and flow boiling combined, while others dedicated entirely to channel flow boiling.

Examples of the first category include articles by Bergles and co-workers covering studies prior to 1980 [31,36], and by Wu and Sundén [37] on studies as recent as 2014. Leong et al. [38] and Shojaeian and Koşar [39] reviewed enhancement of both pool and flow boiling using micro and nano structured surfaces. McCarthy et al. [40], Kim et al. [41], and Attinger et al. [42] reviewed materials as well as methods used to fabricate micro/nanostructured surfaces intended to enhance phase-change heat transfer.

Examples of articles dedicated entirely to channel flow boiling include those by Shatto and Peterson [43], who addressed enhancement attributes of twisted tape inserts, and by Prajapati and Bhandari [44], who explored flow boiling instabilities and their mitigation strategies. Overall, articles addressing enhancement of channel flow boiling exclusively are quite sparse, which is a main motivation for the present review.

1.6. Objectives of present review

This study is a follow-up to a series of recent review articles by the present authors addressing important phase change mechanisms and related fluid flow and heat transfer trends. They include fluid mechanics of liquid drop impact on a liquid film [45] and on a heated wall [46], spray cooling in the single-phase and nucleate boiling regimes (including CHF) [47], and in high temperature boiling regimes and quenching applications [48], mechanisms and models of pool boiling CHF [49,50], pool boiling enhancement techniques using additives and nanofluids [51], and surface modification [52], and macro- and micro-channel nanofluid heat transfer [53].

Unlike most prior boiling enhancement reviews, the present article is dedicated entirely to enhancement of channel flow boiling heat transfer by surface modification, and related operational problems. Included here are separate discussions on macroscale ($\geq$1000 μm), microscale (1–1000 μm), and nanoscale ($\leq$1 μm) surface modifications, in which this simple demarcation is based on enhancement feature size and not channel diameter. Major enhancing mechanisms at different scales of surface modification are extended heat transfer area, increased nucleation sites, and improved capillary wicking for macro, micro and nanoscale, respectively. Carefully addressed for each scheme considered are surface fabrication technique, heat transfer merits (compared to smooth surfaces), and reliability concerns. This article will be concluded with recommendations for future work to address important related mechanisms and implementation issues.

2. Macroscale enhancement ($\geq$1000 μm)

2.1. Cylindrical (Pin) fins

Macroscale surface modifications are adopted to greatly increase heat transfer area as well as enhance mixing of vapor and liquid phases along the flow channel. Three common types of macroscale enhancement are cylindrical (pin) fins, macro ribs, and twisted inserts.

Use of macro pin fins to enhance boiling heat transfer dates back to the mid-1960s, when Haley and Westwater [54] examined single fin performance, and, later, Klein and Westwater [55] showed that optimum fin spacing in extended fin (spline) arrays was equal to bubble departure diameter. Maddox and Mudawar [8] investigated cooling performance for a 12.7 × 12.7-mm^2 device mounted along one wall of a vertical channel. Using FC-72 as coolant and Klein and Westwater's fin spacing criterion, they compared CHF for a smooth surface to one modified with four 5.75-mm diameter and 11.5-mm tall pins, a 6.32 fold increase in surface area. The study explored combining benefits of increasing heat transfer area, flow velocity, and/or subcooling. At velocity of 2.25 m/s and 6.0 °C inlet subcooling, the pin fin surface achieved 6.28 fold increase in CHF compared to the smooth surface, an enhancement virtually equal to the heat transfer area ratio. Heat transfer performance also improved remarkably with increased subcooling. Fig. 2(a) compares vapor growth along the pin surfaces for saturated versus highly subcooled conditions. For the former, upstream portions of the fin tips did not experience any boiling, but a large vapor wake developed downstream. Vapor growth was distinctly different at high subcooling, evidenced by vapor bubbles too small to be detected by the naked eye. Bubble condensation in highly subcooled flow was quite beneficial when stacking a multitude of enhanced surfaces in linear arrangement in the flow channel. Fig. 2(b) compares CHF values for the pin fin surface measured at 2.5 m/s and a broad range of subcoolings to a correlation developed earlier by the same authors [56] for a smooth surface. Strong CHF enhancement with the pin fin surface is shown persisting over the entire subcooling range.

2.2. Macro ribs

Modifying the flow channel with rectangular ribs has been demonstrated to provide moderate CHF enhancement. For example, Kim et al. [57] investigated R-134a CHF enhancement achieved by modifying the inner surface of a 17.04-mm diameter tube with 5.59–8.28-mm wide ribs arranged in helical fashion with 15.46–23.19-mm pitch and 60° helical angle. Overall, CHF improved by 40–60%, depending on rib geometry, operating pressure, and mass velocity. Cheng and Xia [58] measured water flow boiling for an 11.26-mm diameter tube modified with 5.5-mm wide ribs arranged with 3.5-mm pitch and 40° helical angle. They achieved 30–50% CHF enhancement for pressures from 10 to 19 MPa, but the enhancement was insignificant at 21 MPa. Using the same rib configuration but 11.6-mm diameter tube, Cheng and Chen [59] provided useful measurements for water flow boiling heat transfer coefficient and pressure drop.

Kim and Sohn [60] investigated flow boiling heat transfer for R-113 in a vertical 3 × 100-mm^2 rectangular channel with offset strip fins having 2.84-mm hydraulic diameter, and provided correlations for two-phase frictional pressure drop multiplier and local boiling heat transfer coefficient.

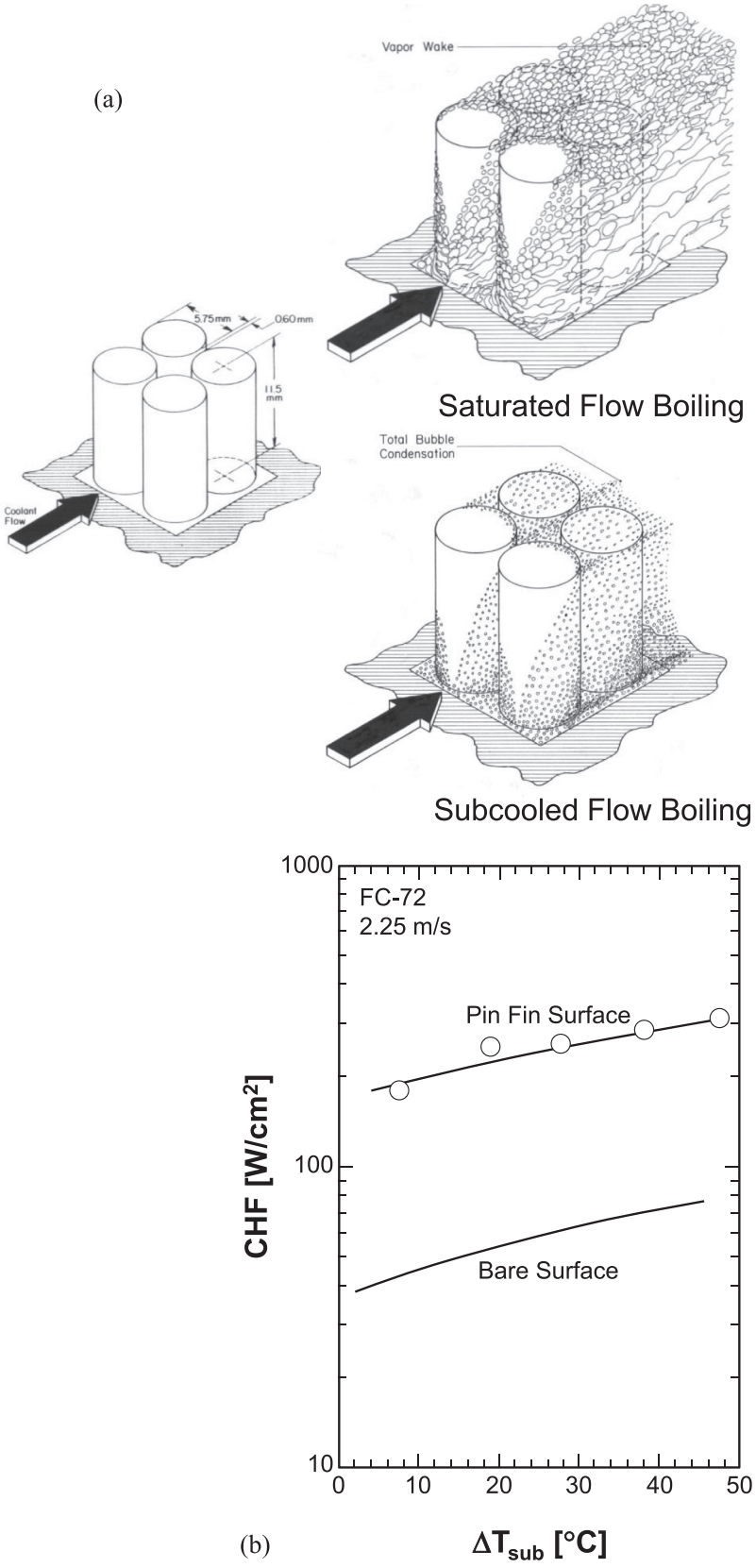

Fig. 2. (a) Comparison of saturated and subcooled channel flow boiling over macro-pin-fins. (b) Comparison of CHF for macro-pin-fin and smooth surfaces over broad range of subcooling. Adapted from Mudawar and Maddox [56].

2.3. Twisted tape inserts

Use of twisted tapes to enhance flow boiling heat transfer in tubes is a bit controversial. On one hand, they do provide several obvious benefits, including improved heat transfer due to increased heat transfer area and better mixing, low cost, and ease of insertion and removal for maintenance [61]. However, they can increase pressure drop appreciably [62,63]. Fig. 3(a) shows flow boiling of R-134a along a twisted tape inserted along a 15.9-mm diameter tube. Kanizawa and Ribatski [64] identified five flow patterns for R-134a flow boiling with twisted tape inserts having twist ratios (defined as 180° turn length divided by tube diameter) from 3 to 14: stratified, stagnant, intermittent, annular-stratified, and annular. Follow-up study by Kanizawa et al. [65] examined heat transfer performance and pressure drop for R-134a in 15.9- and 12.7-mm tubes, and found that lower twist ratios improved heat transfer performance for intermediate vapor qualities. Kanizawa et al. [66] developed a flow pattern based method to predict heat transfer coefficient for flow boiling in a tube containing twisted tapes, but also accounted for swirl flow effects. Agrawal et al. [67] measured both heat transfer coefficient and pressure drop for flow boiling of R-12 in a 10-mm diameter tube. Overall, smaller twist ratios yielded better heat transfer performance, albeit at the expense of higher pressure drop. They correlated pressure drop by modifying the Martinelli-Nelson correlation [68] with a function of twist ratio. Jensen and Bensler [69] found that the benefits of decreasing twist ratio weakened with increasing pressure. Yan et al. [70] reported that twisted tape significantly increased CHF for subcooled water flow boiling in a 9.0-mm diameter tube, and enhancement was more remarkable with smaller twist ratios.

Mogaji et al. [71] devised a criterion under which use of twisted tape inserts was favorable. This criterion is based on magnitude of parameter ε, defined as

$$\varepsilon = \frac{\varepsilon_h}{\varepsilon_{\Delta p}}, \tag{3}$$

where ε_h is *heat transfer enhancement factor*, ratio of heat transfer coefficient for structured (modified) tube to that for bare tube,

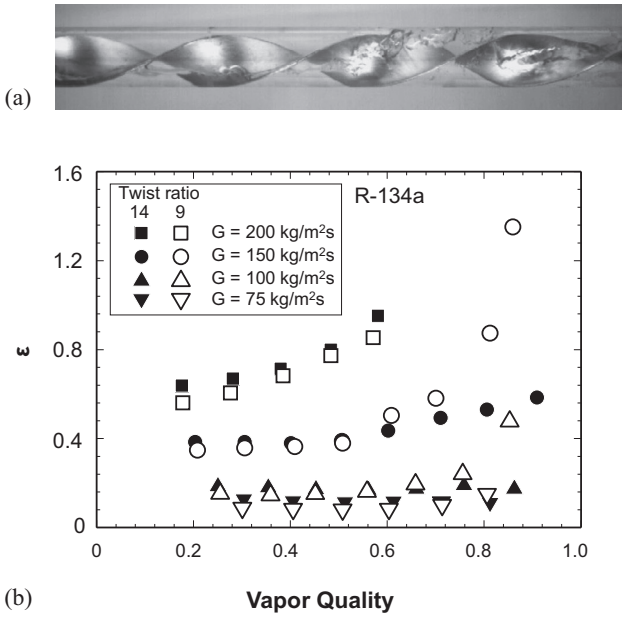

Fig. 3. (a) Flow boiling of R-134a along twisted tape inserted into 15.9-mm tube (adapted from Kanizawa and Ribatski [64]). (b) Variations of ε with thermodynamic equilibrium quality for R-134a for different mass velocities and two twist ratios (adapted from Mogaji et al. [71]).

$$\varepsilon_h = \frac{h_{st}}{h_{pt}}, \tag{4}$$

and $\varepsilon_{\Delta p}$ is *pressure drop penalty factor*, ratio of pressure drop for structured tube to that for plain tube,

$$\varepsilon_{\Delta p} = \frac{\Delta p_{st}}{\Delta p_{pt}}. \tag{5}$$

Fig. 3(b) shows that ε increases with increases in thermodynamic equilibrium quality and mass velocity, which implies that use of twisted tape inserts is more favorable at higher vapor qualities and mass velocities. The same figure shows that, for a mass velocity of 159 kg/m^{2}s , increasing twist ratio from 9 to 14 decreases ε from 1.40 to 0.58.

Inasaka and Nariai [72] evaluated subcooled flow boiling CHF correlations developed prior to 1995 for both bare circular tubes and tubes fitted with twisted tape inserts. Arment et al. [73] modified a correlation by Nariai and Inasaka [74] to predict CHF for tubes with twisted tape inserts. Arment et al. also developed a new methodology for predicting pressure drop inside enhanced tubes. Yagov [75] reported that subcooled boiling heat transfer in swirl flow along a uniformly heated tube can be predicted by superposition of known relations for single-phase convection and nucleate boiling.

Yun et al. [76] examined nitrogen flow boiling at low saturation temperature (−191 °C) for wire coil inserted along a 10.6-mm diameter tube, varying both wire diameter and coil pitch. Tong et al. [77] suggested that swirl flow with twisted tape inserts enhanced heat transfer by reducing thicknesses of wall thermal boundary layer for single-phase flow and bubbly layer for two-phase flow. However, they pointed out that contact thermal resistance between twisted tape and tube wall tended to compromise heat transfer performance. Kinoshita et al. [78] proposed that CHF enhancement with twisted tape inserts was the outcome of alternating initiation and disruption of wall bubble boundary layer.

Overall, macroscale surface modification techniques have demonstrated effectiveness in terms of both flow boiling heat transfer enhancement and ability to maintain stable boiling operation. While macro ribs and twisted tape inserts do provide measurable improvement in performance, best enhancement (especially in CHF) is achieved with macro cylindrical fins. But a key drawback of all three surface modification techniques is relatively large flow diameter, which may be difficult to accommodate in cooling packages subject to stringent volume constraints. Additionally, these macro techniques do not take advantage of the important mechanism of capillary wicking, which is known to improve boiling heat transfer performance by both increasing number of nucleation sites and intensity of boiling from individual sites. This limitation is a primary reason behind recent shift in interest to both microscale and nanoscale surface modification schemes.

3. Microscale enhancement (1–1000 μm)

3.1. Micro-fins (Micro-grooves)

3.1.1. Data trends

Two common types of micro-fins have been incorporated into inner walls of flow channels: *spiral micro-fins*, for circular and rectangular channels, and *pin micro-fins*, for mostly rectangular channels [79].

Filho and Jabardo [80] reported that, at low mass velocities, modifying the inner wall for 9.52-mm diameter and 1.5-mm long copper tubes with micro-fins (also referred to as *micro-grooves*), Fig. 4(a), helped convey liquid upstream, resulting in measurable enhancement in boiling heat transfer coefficient but minimal pressure drop penalty for R-134a compared to a smooth tube. Filho and

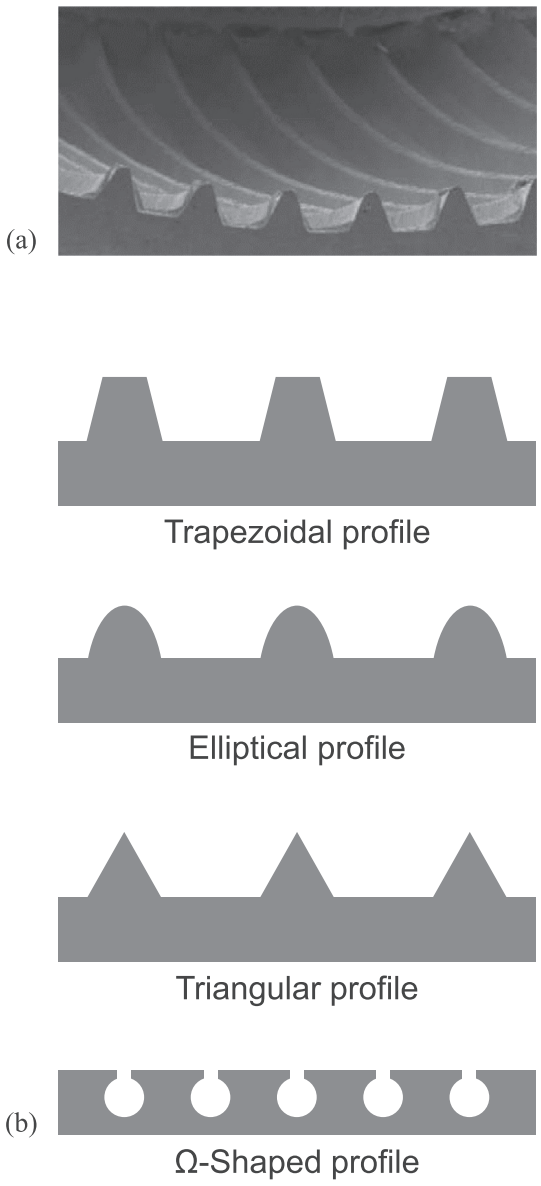

Fig. 4. (a) Cross-sectional view of micro-fin tube employed by Filho and Jabardo [80]. (b) Schematics of micro-fin profiles adopted by various investigators.

Jabardo, and Wellsandt and Vamling [81] investigated flow boiling in herringbone micro-fin tubes. In the latter study, heat transfer coefficient for R-134a was highest at low vapor qualities. Follow-up study by Filho and Barbieri [82] culminated in an enhancement parameter for micro-fin tubes governing both heat transfer and pressure drop that was a function of mass velocity and vapor quality. They showed that high vapor qualities could cause this parameter to fall below unity, indicating inferior heat transfer performance and high pressure drop penalty.

Schlager et al. [83] investigated impact of micro-fin dimensions on heat transfer performance for R-22 in a 12.7-mm tube, with fin height ranging from 150 to 300 μm and spiral angle 15–25°. Kim and Shin [84] and Chamra et al. [85] examined flow boiling of R-22 and R-410A in 15.88-mm tubes modified with two types of micro-fin geometries, single-groove and cross-groove. Spindler and Müller-Steinhagen [86] and Yu et al. [87] found that micro-fin tubes increased wetted surface area for horizontal tubes, thereby assisting transition from stratified wavy flow to annular flow and improving heat transfer performance. Cui et al. [88,89] explored two-phase flow patterns and transitions as well as heat transfer performance of R-134a in micro-fin helically coiled tubes. Soleimani and Keshavarz [90] achieved substantial improvement in subcooled flow boiling heat transfer coefficient with combined use of mini-grooves and nanofluid. Cheng and Chen [91] investigated flow boiling in a tube modified internally with axial micro-grooves. And, Cheng et al. [92] investigated flow boiling heat transfer enhancement in a micro-grooved 15-mm tube at different orientations relative to Earth gravity. The grooves were Ω-shaped, with 1.0-mm groove diameter and inlet width and height of 0.3 and 0.53 mm, respectively.

Abdous et al. [93] investigated effects of fin geometry on flow boiling in a micro-fin tube using entropy analysis, concluding that smaller fin height and width improved performance and reduced entropy generation. They also proved existence of an optimum number of fins for minimum entropy generation, and showed that increasing tube diameter compromised heat transfer performance. Their entropy generation analysis also showed that heat transfer performance of micro-fin tubes improved with increasing saturation temperature and decreases in both mass velocity and inlet vapor quality.

Shown in Fig. 4(b) are examples of micro-fin profiles adopted by various investigators.

3.1.2. Parametric effects

Studies have demonstrated the profound influence of mass velocity on flow boiling heat transfer in tubes. For example, Mancin et al. [94,95] studied R-134a flow boiling in a 3.4-mm micro-fin tube, and showed that CHF increased with increasing mass velocity. But they also pointed out that boiling heat transfer coefficient was independent of mass velocity for wall heat fluxes above 3 W/cm^2, a trend confirmed by Wu et al.'s [96] semi-empirical model covering both intermittent and annular flow patterns. Gao et al. [97] also showed that local heat transfer coefficient for carbon dioxide in a 3.04-mm tube was weakly dependent on mass velocity, indicating that heat transfer was dominated by nucleate boiling rather than convective boiling. However, Padovan et al. [98] found that boiling heat transfer coefficient for both R-134a and R-410A in an 11.6-mm micro-fin tube at relatively high saturation temperatures (30 and 40 °C) increased with increasing mass velocity up to 200 kg/m^{2}s, above which it decreased slightly. Similar non-monotonous influence of mass velocity on heat transfer coefficient was reported by Schael and Kind [99] and Dang et al. [100] for carbon dioxide flow boiling along 9.52- and 2.65-mm diameter micro-fin tubes, respectively. However, Wongsa-ngam et al. [101] showed that heat transfer coefficient for R-134a along 9.52-mm diameter micro-fin tube increased monotonically with increasing mass velocity for values as high as 800 kg/m^{2}s. Singh et al. [102] found that effects of mass velocity on heat transfer coefficient were closely related to changes in flow pattern. Passos et al. [103] pointed out that dominance of nucleate boiling versus convective boiling was tube diameter dependent. Overall, contradictory findings concerning influence of mass velocity on heat transfer performance point to a need for more systematic investigation, taking into account variations in flow pattern and dominant heat transfer mechanism.

In terms of saturation temperature effects, Han et al. [104] showed that heat transfer coefficient and pressure drop for R-161 in a 7-mm diameter micro-fin tube decreased with increasing saturation temperature. Seo and Kim [105] reported similar trend for flow boiling of R-22 in 7- and 9.52-mm micro-fin tubes. However, trends for R-410A by Kim et al. [106] were both tube diameter and heat flux dependent. While their R-410A heat transfer coefficient trend with saturation temperature for the 9.52-mm diameter micro-fin tube agreed with Han et al.'s, the trend for the 7-mm tube was similar only at low heat flux (0.5 W/cm^2), above which

the heat transfer coefficient increased with increasing saturation temperature. Cho and Kim [107] showed that heat transfer coefficient for carbon dioxide in horizontal 5- and 9.52-mm micro-fin tubes increased with increasing saturation temperature. Follow-up study by Cho and co-workers addressed flow boiling heat transfer in vertical [108] and inclined [109] micro-fin tubes, and confirmed the same saturation temperature trend. Kuo and Wang [110] showed that heat transfer coefficient for R-22 in a 9.52-mm diameter micro-fin tube increased with increasing saturation temperature at vapor qualities above 0.2, but temperature had minor influence at lower qualities. Hsieh and Wen [111] reported heat transfer enhancement for R-114 in six rib-type tube annuli with hydraulic diameters ranging from 4.67 to 9.01 mm.

Aside from pure refrigerants, investigators also examined performance of refrigerant/oil mixtures in micro-fin tubes. Hu et al. [112] studied flow boiling of R-410A/oil mixtures in a 7-mm diameter micro-fin tube and reported enhancement in heat transfer coefficient resulting from oil content for vapor qualities below 0.4. However, the oil reduced heat transfer effectiveness for qualities above 0.65, and the heat transfer coefficient deteriorated sharply with increasing oil concentration. Similar trends were reported by Zürcher et al. [113] and Targanski and Cieslinski [114] for R-407C/oil mixtures, Han et al. [115] for R-1234yf/oil mixtures, and Nidegger et al. [116] for R-134a/oil mixtures. Hu et al. [117] showed that oil presence increased pressure drop, and this effect was accentuated at high vapor qualities, which increased local oil concentration. Kondou et al. [118] investigated flow boiling of non-azeotropic R-32/R-1234ze(E) mixture in a horizontal 5.21-mm diameter micro-fin tube and concluded that heat transfer coefficient reached minimum value for 20 wt% R-32 and 80 wt% R-1234ze(E) composition. For both R-22 and R-407C, Kuo and Wang [119] pointed out important differences in flow pattern maps for 9.52-mm diameter micro-fin tube between pure refrigerants and refrigerant/oil mixtures. Diani et al. [120] investigated flow boiling of R1234ze(E) in a 2.4-mm diameter micro-fin tube, and reported that nucleate boiling prevailed at low vapor qualities and high heat fluxes, and convective boiling at high qualities and low fluxes. Their heat transfer coefficient and pressure drop data were successfully predicted using models they developed earlier for a 3.4-mm diameter micro-fin tube [121]; the same models were equally effective at predicting R-1234yf data [122]. They also showed that heat transfer enhancement factor, ε_h, Eq. (4), decreased with increases in mass velocity and heat flux, while pressure drop penalty factor, $\varepsilon_{\Delta p}$, Eq. (5), increased with increasing vapor quality.

Sommers and Yerkes [123] studied flow boiling of R-134a in a rectangular channel having 3×31.75-mm^2 cross-sectional area using three different micro-structure modifications. Shown in Fig. 5(a), two were produced using photolithography and reactive ion etching, and the third laser-ablation. As shown in Fig. 5(b), boiling heat transfer coefficients for the ion etched surfaces were only 35–48% higher than bare surface; whereas, that for the laser-ablated surface was as much as 90–100% higher. Superior performance for the latter was attributed to enhanced nucleation from porous layer of sintered aluminum particles, Fig. 5(c), formed on the surface during the laser ablation. Sommers and Yerkes also reported that boiling performance can be enhanced further by applying a hydrophobic coating to the surface.

Lee et al. [124] performed direct numerical simulation of bubble growth and heat transfer for water flow boiling in a micro-fin rectangular channel having 0.2×1.0-mm^2 cross-sectional area.

3.1.3. Predictive methods

Yun et al. [125] developed a generalized correlation for flow boiling heat transfer coefficient in micro-fin tubes by modifying a prior smooth tube correlation with dimensionless parameters to account for surface modification; their approach was validated against 749 data points for five refrigerants and two fin shapes. Honda and Wang [126] and Makishi et al. [127] proposed a stratified annular flow model for evaporation heat transfer in horizontal micro-fin tubes, accounting for contributions of thin film evaporation, nucleate boiling, and forced convection. Zhang and Yuan [128] developed a predictive methodology for evaporation heat transfer of refrigerant mixtures in micro-fin tubes. More recently, Merchant and Mehendale [129] presented a model to predict heat transfer coefficient for flow boiling in horizontal micro-fin tubes using a database for different fluids from prior literature consisting of 1576 data points.

Overall, available predictive methods are quite empirical and arrived at by modifying correlations or models developed previously for plain surfaces. Aside from the multiple parameters affecting flow boiling heat transfer (even for plain surfaces) and poor understanding of underlying mechanisms, heat transfer on enhanced surfaces is complicated further by the various geometries used and multiple feature sizes of surface structures. These complications render modeling heat transfer on enhanced surfaces quite challenging.

3.2. Micro-studs and square micro-fins

Aside from the macro pin fins discussed earlier, Maddox and Mudawar [8] investigated enhanced flow boiling heat transfer of FC-72 from 12.7×12.7-mm^2 heating surface flush mounted to one wall of a vertical 12.7×38.1-mm^2 rectangular channel. The surface was modified using three different square micro-studs having equal width and spacing of 0.305 mm and heights of 0.25, 0.51, and 1.02 mm, which, as shown in Fig. 6(a), were orientated at 45° relative to the coolant flow. Their tests showed monotonic increase of heat transfer performance with increasing stud height, as shown in Fig. 6(b). Follow-up study by Mudawar and Maddox [24] compared heat transfer performances of three different enhancement schemes, 45° micro-stud, micro-groove (oriented parallel to flow direction), Fig. 6(c), and the 11.7-mm tall pin fins depicted earlier in Fig. 2. Overall, best performance was achieved at 4.1 m/s coolant velocity and high subcooling of ΔT_{sub} = 44.9–48.9 °C, which culminated in CHF values of 126 W/cm^2 for the bare surface, and 262, 317, and 361 W/cm^2 for the 1.02-mm tall 45° micro-stud, 1.02-mm tall micro-groove, and pin fin, respectively; the latter three were 2.08, 2.52, and 2.87 times bare surface CHF. They also correlated bare and enhanced surface CHF data using a model they developed earlier based on the Haramura and Katto [130] macro-layer dryout mechanism. Despite achieving highest CHF with the macro pin fin surface, they suggested that the micro-stud and micro-groove surfaces, which yielded lower CHF values, might be preferred for applications with stringent cooling module volume requirements.

Contrary to the findings of Maddox and Mudawar, McNeil et al. [131] reported that heat transfer coefficient for R-113 in a 1×50-mm^2 rectangular channel with bottom surface modified with 1-mm wide and tall square fins was only slightly larger than for a bare surface, but the former yielded a 7-fold increase in pressure drop.

Lee et al. [132,133] proposed an enhancement technique for water consisting of parallel rectangular 539-μm diameter micro-channels with 26.6° oblique fins in between. This configuration improved single-phase heat transfer by re-initiating both hydrodynamic and thermal boundary layers at leading edge of each oblique fin, effectively reducing overall boundary layer thickness and promoting better mixing. In follow-up study, Law et al. [134] extended this concept to flow boiling of FC-72 in 0.3×1.2-mm^2 rectangular micro-channels, reporting that heat transfer was dominated by nucleate boiling at low heat fluxes, transitioning to convective

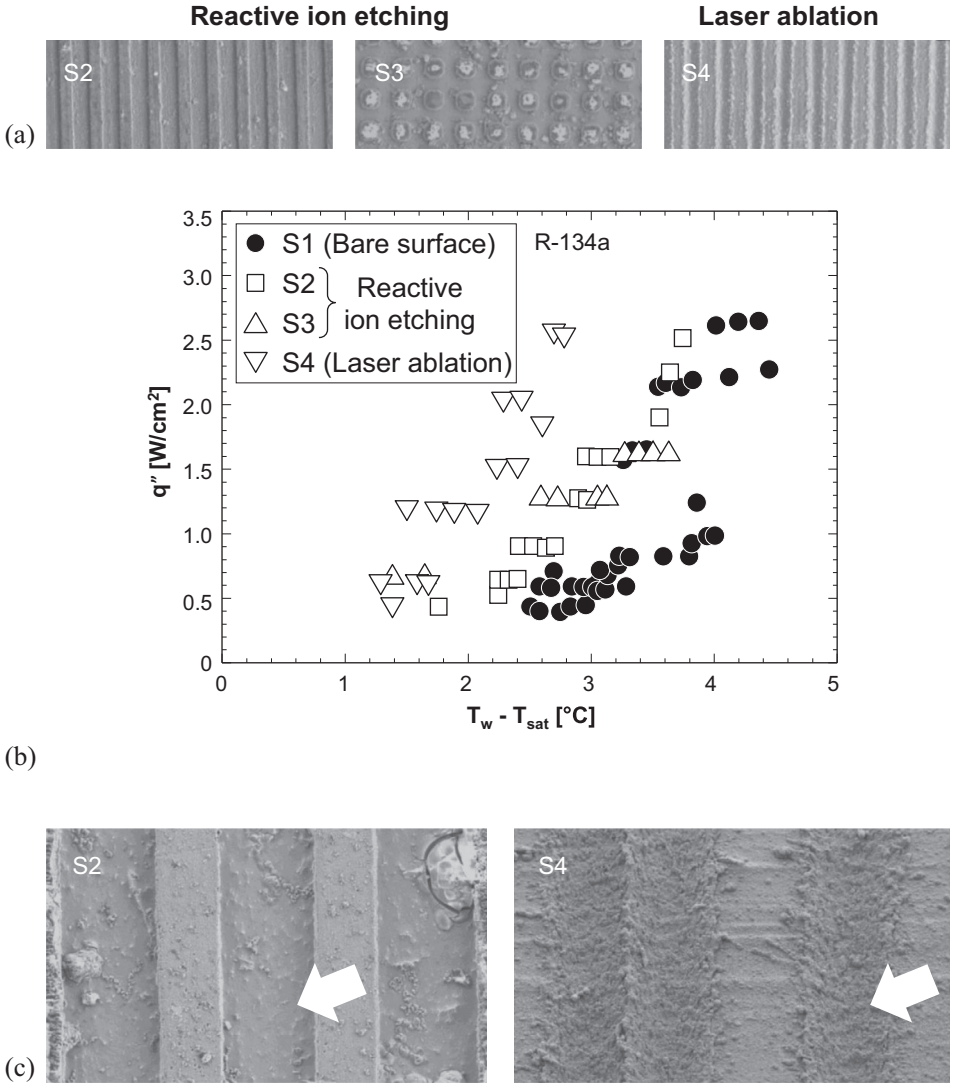

Fig. 5. (a) SEM images of micro-structured surfaces. (b) R-134a flow boiling curves for different surfaces. (c) Magnified SEM images of micro-structured surfaces (S2 and S4 from (a)). Adapted from Sommers and Yerkes [123].

boiling (via thin-film evaporation) at medium heat fluxes, and convective boiling at high heat fluxes leading to CHF. Law and Lee [135] compared FC-72 flow boiling performances of straight-fin and oblique-fin micro-channels, and achieved with the latter 6.2 and 2.8 times improvements in heat transfer coefficient and CHF, respectively, while incurring 1.7 times increase in pressure drop. They postulated that oblique fins offered improved performance by reducing wall temperature gradients and pressure fluctuations. They added that constant shearing and breaking of large bubbles and slugs by sharp corners of oblique fins helped minimize vapor buildup along the micro-channels. Overall, increased bubble generation rate in the nucleate boiling region and a continuously developing thin liquid film in the convective boiling region served as major contributions to heat transfer enhancement with oblique fins.

Cognata et al. [136] examined flow boiling heat transfer of R-11 on staggered 150-μm square fins orientated 45° relative to flow direction, and pointed out absence of any flow instabilities with this scheme. Reeser et al. [137] investigated flow boiling heat transfer from staggered and inline square micro-fin arrays with fin width and height of 0.153 and 0.305 mm, respectively, using deionized water and HFE-7200 as working fluids, with exit qualities up to 90% to develop modified correlations for heat transfer coefficient and pressure drop. Qu and Siu-Ho [138] studied saturated flow boiling heat transfer of water from an array of staggered square micro-fins with fin width and height of 0.2 and 0.67 mm, respectively, and identified dominant heat transfer mechanisms associated with annular flow. In a parallel study, Qu and Siu-Ho [139] also examined pressure drop using the same enhancement scheme. They showed that, when used in conjunction with a modified single-phase friction factor correlation, the Lockhart-Martinelli correlation for laminar liquid and laminar vapor provided good prediction of pressure drop data.

Woodcock et al. [140] and Yu et al. [141,142] devised a 'piranha' pin-fin structure with 150-μm feature size in a 0.5 × 2.4-mm^2 rectangular micro-channel in pursuit of increased heat transfer area, increased nucleation site density, and more effective release of vapor bubbles. Using a relatively high mass velocity of 2460 kg/m^{2}s, they achieved a CHF for HFE-7100 of 676 W/cm^2, and reported that both heat transfer coefficient and pressure drop were influenced by width of piranha mouth opening. Krishnamurthy and Peles [143] studied water flow boiling in a 0.25 × 1.8-mm^2 rectangular micro-channel enclosing staggered micro-pin-fins with 100-μm diameter and 250-μm height. They showed that heat transfer

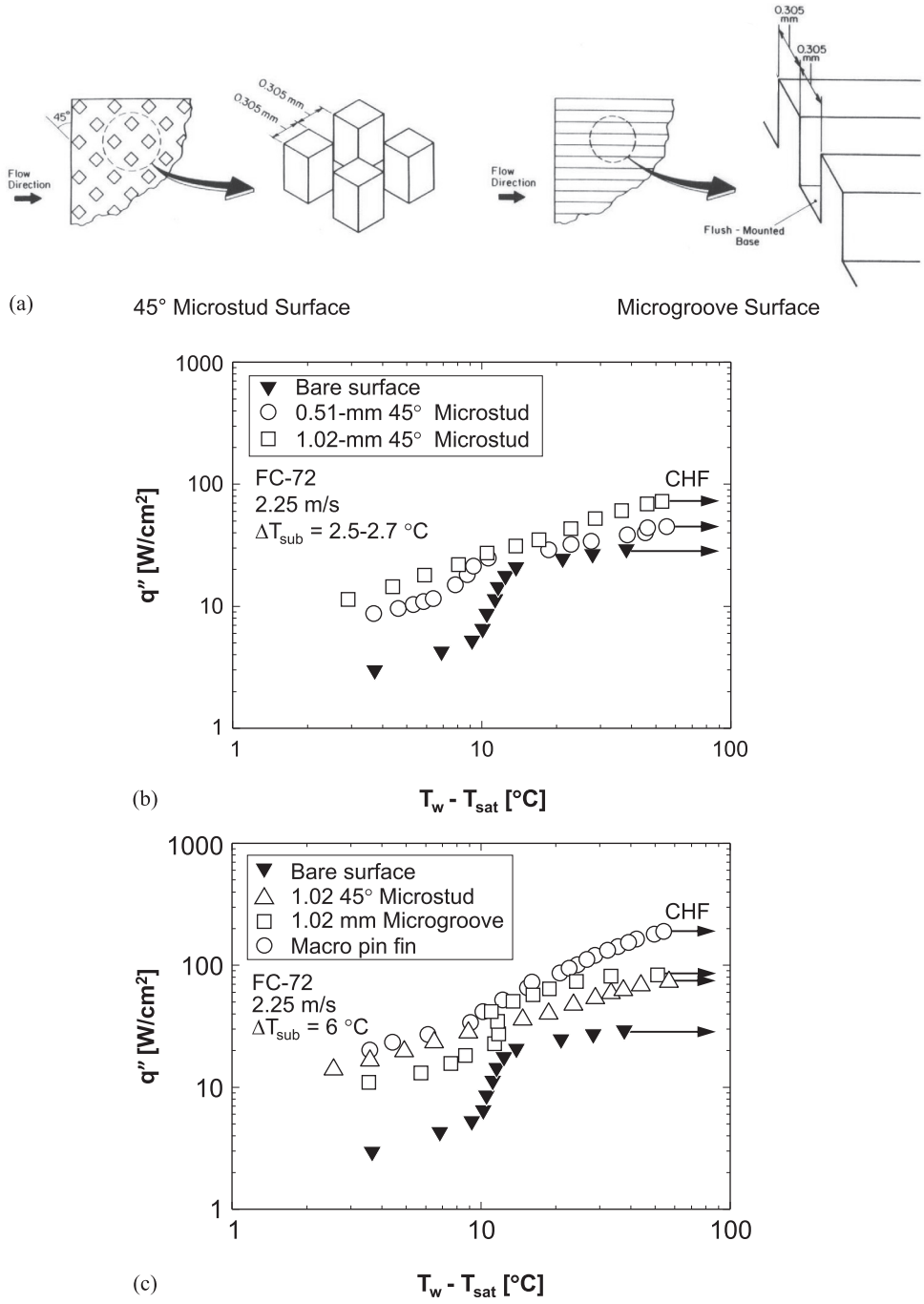

Fig. 6. (a) Schematics of micro-stud and micro-groove enhanced surfaces. (b) Effects of micro-stud height on boiling performance for FC-72 (adapted from Maddox and Mudawar [8]). (c) Comparison of FC-72 flow boiling performances for bare, micro-stud, micro-groove, and macro-pin-fin surfaces (adapted from Mudawar and Maddox [24]).

coefficient for water was moderately dependent on mass velocity but independent of heat flux, which pointed to heat transfer performance dominated by convective boiling. Their follow-up work [144,145] addressed bubble behavior and flow patterns for HFE-7000 flow boiling in 222-μm hydraulic diameter rectangular micro-channels modified each with a single row of 24 inline 100-μm diameter pin-fins. Koşar and Peles [146] also proposed a surface having hydrofoil-based micro-pin-fins with 1030-μm wetted perimeter and 100-μm chord thickness to enhance flow boiling. Using this scheme, heat transfer coefficient for R-123 increased with increasing heat flux, acquiring maximum value before declining until reaching CHF, which was triggered mostly by dryout.

Ma et al. [147] and Yuan et al. [148] used dry etching to fabricate square micro-fins with 30- and 50-μm widths and 60- and 120-μm heights on a chip surface, which they used to enhance flow boiling heat transfer for FC-72. They reported that CHF for the finned surfaces was more sensitive to fluid velocity and subcooling than the smooth, but nucleate boiling region of the boiling curve was virtually independent of the same parameters. Lie et al. [149] and Chang et al. [150] showed that forming square micro-fins with 100- and 200-μm widths and 70-μm height on a chip surface offered the advantages of decreased bubble departure diameter and increased departure frequency for FC-72.

Deng et al. [151] fabricated conical micro-fins on the bottom surfaces of 750-μm hydraulic diameter rectangular micro-channels using laser micro-milling. This structure was effective at enhancing flow boiling heat transfer coefficient for both water and ethanol, improvement they attributed to abundance of tiny reentrant cavities and to liquid rewetting by this surface's strong wicking effects. The same scheme also mitigated severe two-phase flow instabilities sometimes encountered in conventional micro-channel heat sinks. Using water as coolant, Wan et al. [152] compared thermal performances of four types of staggered micro-fins with different cross-section shapes: square, circular, diamond, and streamline. The square micro-fins yielded best boiling heat transfer performance, followed by circular, streamline, and diamond. Additionally, the square and circular micro-fins showed added superiority in terms of mitigation of two-phase flow instabilities. These observations pointed to square micro-fins as optimum overall choice for flow boiling enhancement.

Zhu et al. [153,154] designed and fabricated arrays of 5- to 10-μm diameter and 25-μm high silicon micro-pillars on the bottom wall of a $0.5 \times 0.5\text{-mm}^2$ micro-channel to promote capillary flow for thin film evaporation while facilitating nucleation only from the sidewalls. Results for water showed significant reduction in wall temperature and pressure drop fluctuations, especially at high heat fluxes, and CHF values as high as $969\ \text{W/cm}^2$, a 57% enhancement compared to smooth surface. Bigham et al. [155] attempted to explain the mechanisms governing heat transfer enhancement for water flow boiling on micro-pin–fin surfaces in a $0.075 \times 0.25\text{-mm}^2$ rectangular micro-channel using a model incorporating effects of three parameters: drying time scale for liquid film wicking into surface structures, heating length scale of liquid film, and area fraction of evaporating liquid film.

3.3. Artificial cavities

Surface texture has always been considered important to not only boiling but radiation heat transfer as well [156]. For flow boiling, a primary goal is to increase number of active bubble nucleation sites using mostly reentrant cavities. For example, Kuo and Peles [157] showed, using HFE-7000, that reentrant cavities on sidewalls of $0.2 \times 0.25\ \text{mm}^2$ rectangular micro-channels reduced wall superheat at onset of boiling and increased flow boiling heat transfer coefficient by 30% compared to channels without cavities, albeit without influencing CHF. However, they pointed out diminution in the enhancement at high qualities where convective boiling prevailed. But, unlike the HFE-7000 results, they showed that use of reentrant cavities in identical micro-channels improved CHF for water [158]. Koşar et al. [159] encountered both nucleate and convective boiling dominant regimes for R-123 flow in 227-μm hydraulic diameter rectangular micro-channels modified with 7.5-μm wide interconnected reentrant cavities, and established a criterion for transition between the two regimes based on Reynolds and Boiling numbers. Follow-up study by Koşar et al. [160] addressed performance of the same enhancement scheme at a reduced pressure of 47 kPa, and showed that transition from nucleate to convective boiling occurred at lower Reynolds and Boiling numbers than at atmospheric pressure. Lin et al. [161] investigated flow boiling heat transfer and CHF for methanol-water mixtures in a diverging rectangular micro-channel (85-μm high with 540-μm inlet width and 760-μm outlet width) modified with artificial cavities with 15-μm mouth diameter. Flow visualization results showed that Marangoni effect moved liquid towards the contact line, thereby improving heat transfer performance; this effect was incorporated into their empirical correlation for CHF.

Piasecka [162–164] used liquid crystal thermography to measure temperature of FC-72 flow boiling along heated wall of a $1 \times 40\ \text{mm}^2$ rectangular channel that was modified with cavities 1-μm deep, and reported earlier boiling inception compared to plain surface. Li et al. [165] showed that forming triangular cavities 50-μm deep in a $0.2 \times 0.2\ \text{mm}^2$ micro-channel presented several important benefits for acetone, including significant enhancement of heat transfer coefficient, reduction of pressure drop, and more stable and uniform wall temperature compared to a channel without cavities. Rioboo et al. [166] devised a chemical technique to control position of active nucleation sites by grafting the heated surface with alkylsilane self-assembled monolayers. They showed that bubbles in water remained localized atop the grafted zone and center of mass of bubble zone only moved along the vertical axis, without lateral drift.

Zeng et al. [167] modified micro-grooved channels with reentrant cavities using an orthogonal 'ploughing/extrusion' method, and achieved higher boiling heat transfer coefficients for water than channels without cavities, which they attributed to both enhanced nucleation and boundary layer interruption. This scheme also helped mitigate two-phase instability by sharp corners of cavities and capillary-driven liquid intake, albeit at the expense of higher pressure drop. Sitar and Golobic [168] devised an enhancement scheme consisting of interconnected rectangular micro-channels with 25–80 μm hydraulic diameter that were modified with artificial cavities with feature size in the range of 2–12 μm. They were able to increase heat transfer coefficient for water by 3–10 times depending on size of etched cavities and heat flux level. They also reported that the same scheme helped reduce flow boiling instabilities. Hsieh and Lin [169] studied flow boiling in $0.2 \times 0.2\ \text{mm}^2$ micro-channels with sidewall pyramidal cavities at different angles and bottom wall sputtered with 2-μm thick diamond film. By testing water, MCNT-water solution, and FC-72, they concluded that maximum enhancement in flow boiling performance was achieved with a cavity angle of 90°.

3.4. Porous coating and foam

Both porous coatings on channel walls and foams formed into channels have been used to improve flow boiling heat transfer by increasing both nucleation site density and heat transfer area. Ammerman and You [170] and Rainey et al. [171] applied microporous coating along walls of 2-mm and 12.7-mm wide square channels. Using both FC-87 and FC-72, they showed that this scheme led to boiling initiation at lower wall superheat and enhanced both heat transfer coefficient and CHF. Additionally, these enhancements were insensitive to flow velocity, which was opposite to performance of channels without the coating, where heat transfer performance improved steadily with increasing velocity, eventually surpassing performance of the coated channel. Applying different coating materials and particle sizes, Fig. 7(a), along the inner wall of a circular 10.92-mm diameter tube, Sarwar et al. [172] showed that water flow boiling CHF enhancement was greater for microporous than nanoporous coatings, as shown in Fig. 7(b) and 7(c) for subcoolings of 75 °C and 50 °C, respectively. They attributed these performance differences to improved surface wettability on the microporous coating, compared to insignificant improvement on the nanoporous, outcome of nanoparticle agglomeration. Sarwar et al. also reported that the nanoporous coating did not possess sufficient adhesion strength to sustain performance during flow boiling experiments.

Pranoto and Leong [173] studied bubble behavior and flow boiling heat transfer for FC-72 in a 2-mm high channel filled with porous graphite foam. They tested two foam types, 'Pocofoam', having 61% porosity, and 'Kfoam', 72%, and reported enhancement in nucleate boiling heat transfer coefficient by up to 2.5 and 1.9 times, respectively, compared to the channel without foam, but did not address pressure drop penalty. Zhao et al. [174] investigated flow boiling of R-134a in a 26-mm diameter tube filled with metal foam.

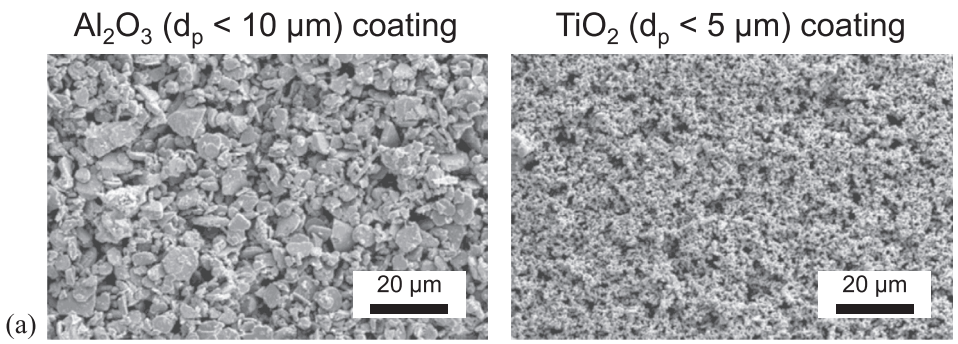

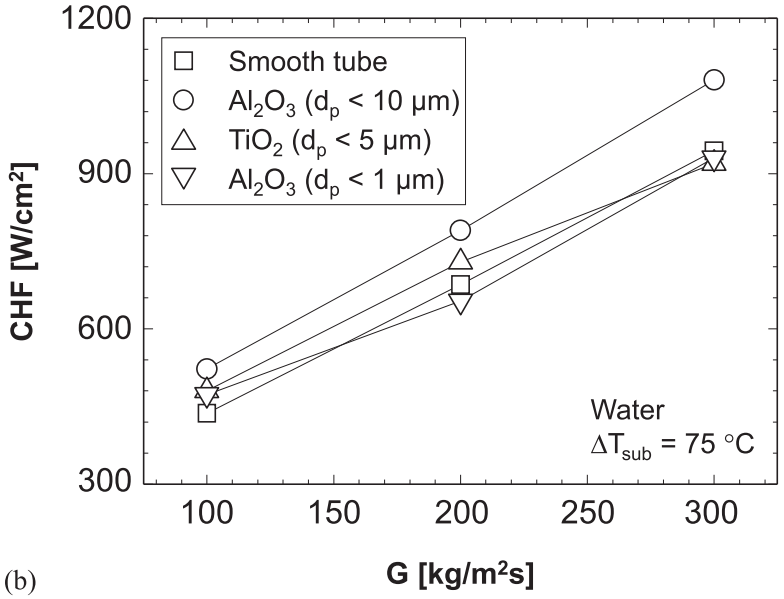

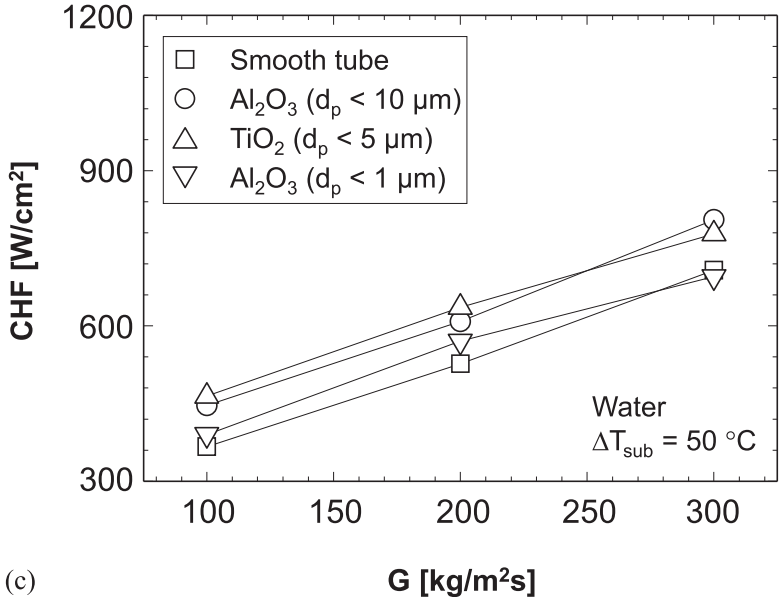

Fig. 7. (a) SEM images of micro-porous coatings, and variations of water CHF with mass velocity for different coating materials and particle sizes for (b) 75 °C and (c) 50 °C subcooling. Adapted from Sarwar et al. [172].

Both heat transfer coefficient and pressure drop showed strong dependence on foam cell size, doubling as cell size was decreased from 20 to 40 ppi.

Chen et al. [175] studied flow boiling heat transfer for water in $10 \times 30\ mm^2$ rectangular channels packed with sintered bi-dispersed porous copper and achieved earlier boiling inception, which they attributed to increases in both heat transfer area and number of nucleation sites. They also compared performances of bi- and mono-dispersed porous media.

After proposing use of solid copper micro-channels modified with Ω-shaped reentrant cavities (see Fig. 4(b)) [176], Deng et al. [177–179] devised a solid-state sintering technique to form

Ω-shaped cavities in porous micro-channel walls. Compared to non-porous solid copper micro-channels with Ω-shaped cavities, the sintering decreased flow boiling incipience superheat and improved bubble nucleation for water. Additionally, two-phase heat transfer coefficient was significantly enhanced for low to moderate heat fluxes, but was inferior to that for non-porous micro-channels at high heat fluxes [180]. A major drawback of the solid-state sintering method was susceptibility to severe two-phase flow instabilities at moderate heat fluxes [181]. Recent work by Deng et al. [182] involving use of interconnected Ω-shaped cavities showed improved ability to mitigate two-phase flow instabilities as well as better stream-wise temperature uniformity for both water and ethanol.

Bai et al. [183] investigated ethanol flow boiling in parallel 0.54-mm hydraulic diameter micro-channels porous-coated using the copper particle sintering technique. While the coating caused a slight increase in pressure drop, it did provide significant mitigation of pressure drop fluctuation. The coating also yielded significant enhancement of flow boiling heat transfer coefficient, particularly at low vapor qualities, and the enhancement was copper particle size dependent. Sun et al. [184,185] addressed the effects of copper particle size and coating thickness on flow boiling performance of FC-72 in 0.49–1.26-mm hydraulic diameter rectangular channels also porous-coated using the sintering method.

Zhang et al. [186] and Tang et al. [187] used wire electric discharge machining to construct a network of interconnected orthogonally-piled 0.4×1.1-mm^2 micro-channels, which yielded 0.4-mm square pores. This scheme both improved heat transfer coefficient and decreased pressure drop for water at 10 °C and 40 °C subcoolings compared to traditional rectangular micro-channels, but the same advantages were not realized at 70 °C subcooling. Another advantage of the interconnected micro-channels was significant mitigation of two-phase flow instabilities. Follow-up study by Zhang et al. [188] showed that heat transfer performance of the same enhancement scheme was superior to that of conventional micro-channels only at low mass velocities. Zhang et al. [189] also investigated water flow boiling in a network of interconnected 0.25–0.55-mm wide micro-channels having porous walls modified using copper powder sintering. Megahed [190] found that cross-linked 248-μm hydraulic diameter micro-channels increased number of active nucleation sites and enhanced uniformity of both fluid flow and surface temperature compared to conventional micro-channels.

Wang and Peterson [191] investigated flow boiling of HFE-7000 in 0.51×1-mm^2 rectangular micro-channels having walls modified with diffusion-brazed fine metal wire mesh screen. This method yielded early boiling inception as well as improvements in both heat transfer coefficient and CHF, without apparent pressure drop penalty. Dawidowicz and Cieśliński [192] applied porous coating on the inner wall of an 8.8-mm diameter tube, and achieved higher boiling heat transfer coefficient and lower pressure drop than a smooth tube for R-22, R-134a, R-407C, and mixtures thereof with polyester oil. Cui et al. [193] used a two-step electro-deposition method to form microporous surface in a square 30×30-mm^2 channel and showed improvement in water flow boiling. This scheme produced hydrophobic cauliflower-like structured surface in the first step, which changed to hydrophilic honeycomb-like in the second step.

Recently, Palko et al. [194] integrated laser-etched polycrystalline diamond micro-channels with template-fabricated microporous copper to enhance convective boiling. The triangular micro-channels had both height and base width of 500 μm. Using water as coolant, this structure had the potential to dissipate 5000 W/cm^2 over a 200×200-μm^2 area, with a temperature nonuniformity of less than 3 °C.

3.5. Other techniques

Aside from the above-mentioned categories of microscale techniques for augmenting flow boiling heat transfer, several others have been proposed. Fu et al. [195] reported that saw-tooth structures formed on bottom walls of 0.5×2-mm^2 rectangular channels helped interrupt thermal boundary layer development and inhibit bubble coalescence for HFE-7100, which improved CHF. Chung and Pan [196] achieved 46.7 and 40.2% improvement in CHF for HFE-7100 with parallel and counter saw-tooth structures, respectively, at 127 kg/m^{2}s mass velocity. However, at a higher mass flux of 285 kg/m^{2}s, no CHF improvement was realized with the parallel configuration and only 17.1% with the counter. Cao et al. [197] investigated a cavitation structure configured in a 0.5-mm deep and 0.5–3-mm wide micro-channel. They showed that flow boiling of R-134a began at the cavitation structure, and this enhancement scheme helped maintain stable flow boiling.

Ahn et al. [198] used anodic oxidation to produce micro-structures along inner wall of a 9.52-mm diameter tube made from Zirlo, a zirconium alloy employed in nuclear fuel cladding. Capillary wicking in the micro-structured surface provided complete wetting and liquid spreading. This important attribute is captured in Fig. 8(a), where the image to the left shows a water drop on untreated tube wall and to the right on micro-structured. Shown in Fig. 8(b) are SEM images of the modified Zirlo micro-structure. Ahn et al. found that water CHF enhancement increased with increasing mass velocity but had weak dependence on fluid inlet temperature, as shown in Fig. 8(c).

4. Nanoscale enhancement (≤1 μm)

4.1. Carbon nanotubes

Carbon nanotubes (CNTs) are extremely thin tubes of graphitic carbon with outer diameters ranging from 1 to 100 nm and lengths from 1 to 50 μm. During the past decade, CNTs have been adopted as coating material for flow boiling enhancement by capitalizing on both their extraordinary high thermal conductivity and superior mechanical properties.

Khanikar et al. [199] assessed heat transfer benefits of coating CNTs upon the bottom wall of a shallow rectangular micro-channel having 0.371×10-mm^2 cross-section and length of 44.8 mm. Using water as working fluid, boiling commenced in the downstream region of the channel. Fluctuations in both inlet and outlet pressure intensified with increasing heat flux, especially near CHF, which was triggered by vapor backflow into the upstream plenum, resulting in dryout over much of the heated surface [200]. Enhanced by increased surface area resulting from the CNT coating, CHF was fairly repeatable at low mass velocities but degraded following repeated tests at high mass velocities because of appreciable morphological changes to the CNT-coated wall. They observed that initially near-vertical CNTs became bent upon the heated surface at high mass fluxes to form a ‘fish scale’ pattern, as shown in Fig. 9(a) and (b). Voids between the fish scales provided near-zero-angle cavities that aided bubble nucleation. Fig. 9(c) shows the degradation in CHF following repeated tests, which was attributed to bending and folding of CNTs upon the coated wall. Similar CHF degradation was reported by Kumar et al. [201] for flow boiling at higher mass velocities in a 0.4×20-mm^2 rectangular channel whose bottom wall was coated with CNTs in which adhesion to the copper wall was enhanced with use of an intermediate diamond layer. Singh et al. [202] investigated water flow boiling in a 10×10-cm^2 channel having a bottom wall coated with CNTs, and reported enhancement in flow

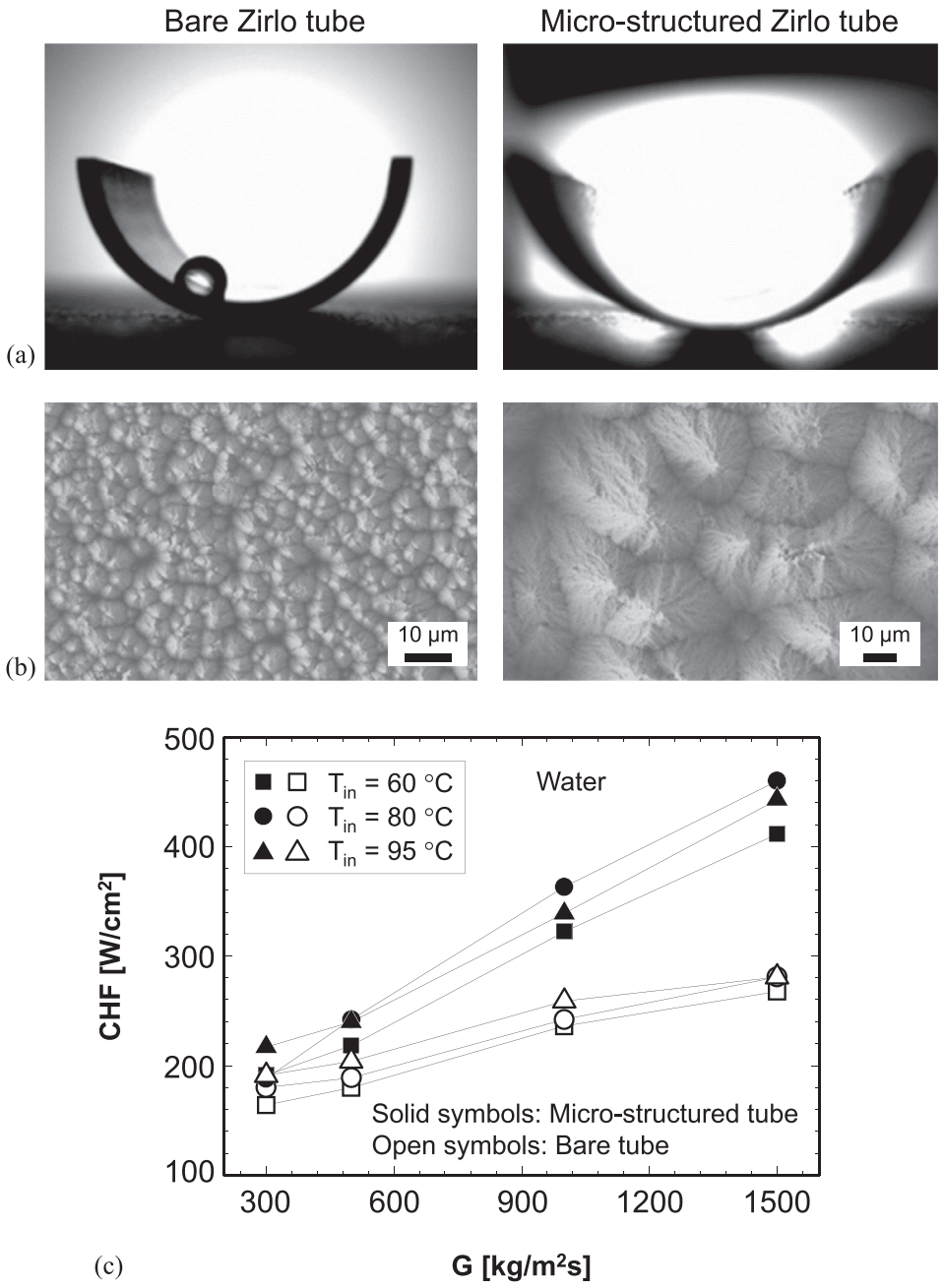

Fig. 8. (a) Water drop formation on inner wall of 9.52-mm Zirlo tube without anodic oxidization (left) and with oxidization (right). (b) SEM images of micro-structured tube surface. Variations of water CHF with mass velocity for different inlet temperatures. Adapted from Ahn et al. [198].

boiling performance mostly at low mass velocities and subcoolings; they too encountered CHF degradation at high mass velocities. Overall, available findings point to a need for careful assessment of time dependent heat transfer performance not only for CNT-coated channels, but nanoscale enhancement techniques in general.

Kousalya et al. [203] investigated water flow boiling from a CNTs-coated copper surface in a rectangular 5.5-mm high channel. They performed experiments with and without exposing the coated surface to low-intensity ultraviolet–visible excitation. Compared to non-illuminated tests, average boiling incipience superheat decreased by 4.6 °C and heat transfer coefficient improved by 41.5%; this augmentation was attributed to hydrophilicity and possible nanoscale optothermal effects.

4.2. Nanowires

Nanowire is defined as a nanoscale rod having a diameter of tens of nanometers and large length-to-diameter ratio. Morshed et al. [204] studied flow boiling of FC-72 in a rectangular 672-μm hydraulic diameter micro-channel in which heating surface was coated with copper nanowire. Despite improvement in heat transfer coefficient and only minor changes to pressure drop, this scheme failed to manage flow boiling instability. On the other hand, Li et al. [205] showed experimentally that coating heating surface of a 0.2 × 0.25-mm^2 rectangular channel with silicon nanowire, which was produced using a monolithic micro/nano fabrication process, did suppress water flow boiling instability and augment heat transfer performance, the latter evidenced by early

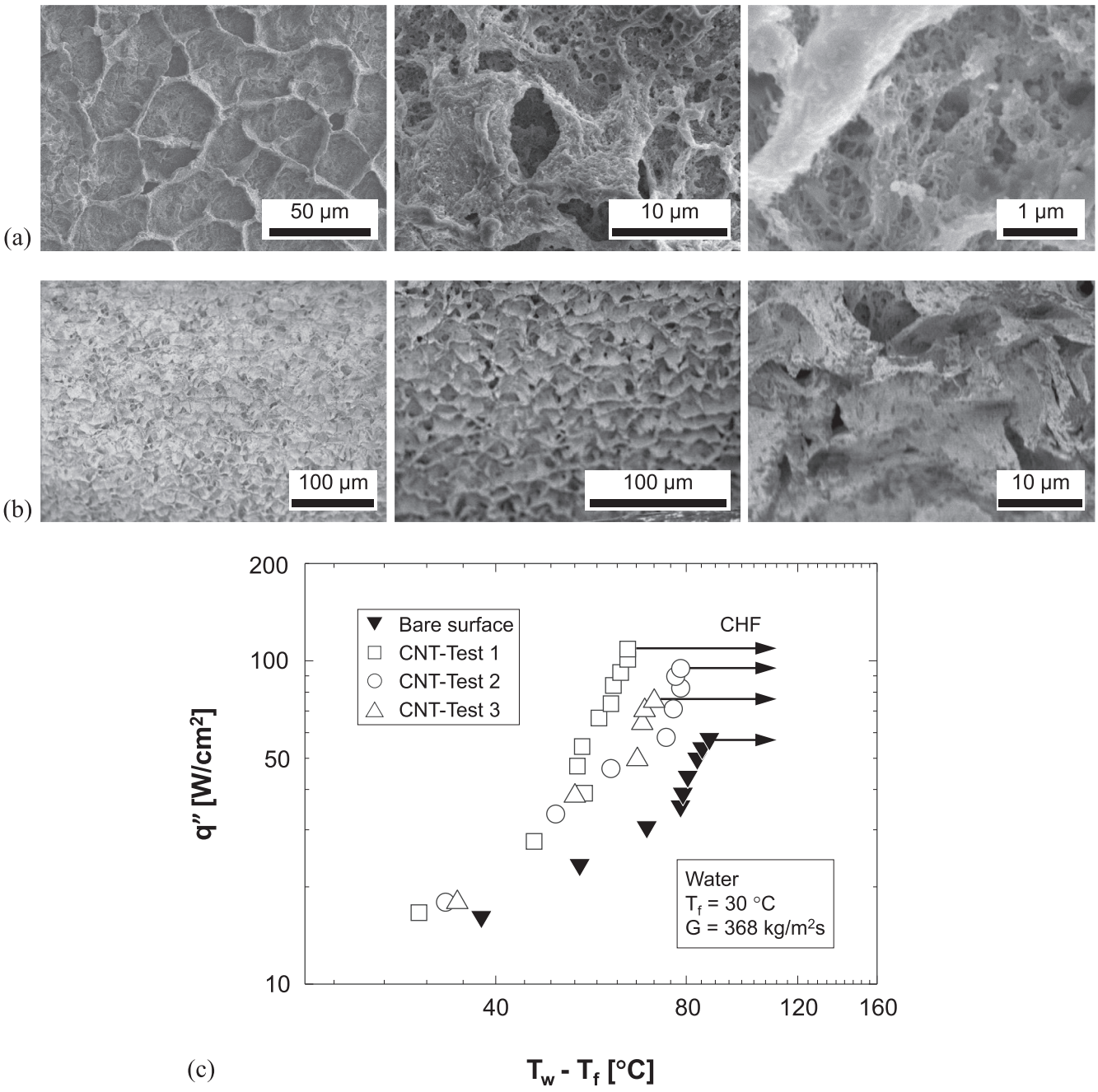

Fig. 9. (a) SEM images of cellular CNT formations over isolated regions of coated surface. (b) Dominant 'fish-scale' pattern observed over most of CNT-coated surface after five boiling tests. (c) Changes in subcooled water flow boiling curve at $G = 368$ kg/m^{2}s and $T_{in} = 30$ °C in three repeatability tests. Adapted from Khanikar et al. [199].

onset of nucleate boiling and improved heat transfer coefficient. Overall, flow oscillations were delayed and amplitudes of temperature and pressure drop oscillations suppressed. Yang et al. [206] studied flow boiling of HFE-7000 in a 0.22×0.25-mm^2 channel in which heating surface was coated with silicon nanowires, SEM images of which are shown in Fig. 10(a). For mass velocities between 1018 and 2206 kg/m^{2}s, they achieved up to 344% enhancement in heat transfer coefficient, result of improvements in both nucleation and evaporation, and up to 40% reduction in pumping power; the latter was attributed to capillary-enhanced phase separation. Shown in Fig. 10(b) and (c) are comparisons for heat transfer coefficient and pumping power, respectively, between coated and plain surfaces. In the same experiments, CHF was enhanced by up to 14.9% at 1018 kg/m^{2}s but decreased at higher mass velocities. Prior work by Yang et al. [207,208] also included water flow boiling results for same channel dimensions and silicon nanowire coating corresponding to the annular regime in which three dominant modes for heat transfer were identified: nucleate boiling, thin film evaporation, and liquid film renewal.

Alam et al. [209] also investigated water flow boiling in a rectangular 0.22×0.25-mm^2 channel in which heating surface was coated with silicon nanowires. They attributed observed surface rewetting and higher CHF to higher surface tension force at the liquid-vapor interface and capillary effects provided by the nanowires. Their parallel study [210] showed that strong surface tension effects at the liquid-vapor interface of growing bubbles led to higher heat transfer contact area, lower thermal resistance, and better thin film evaporation. On the other hand, inertia was

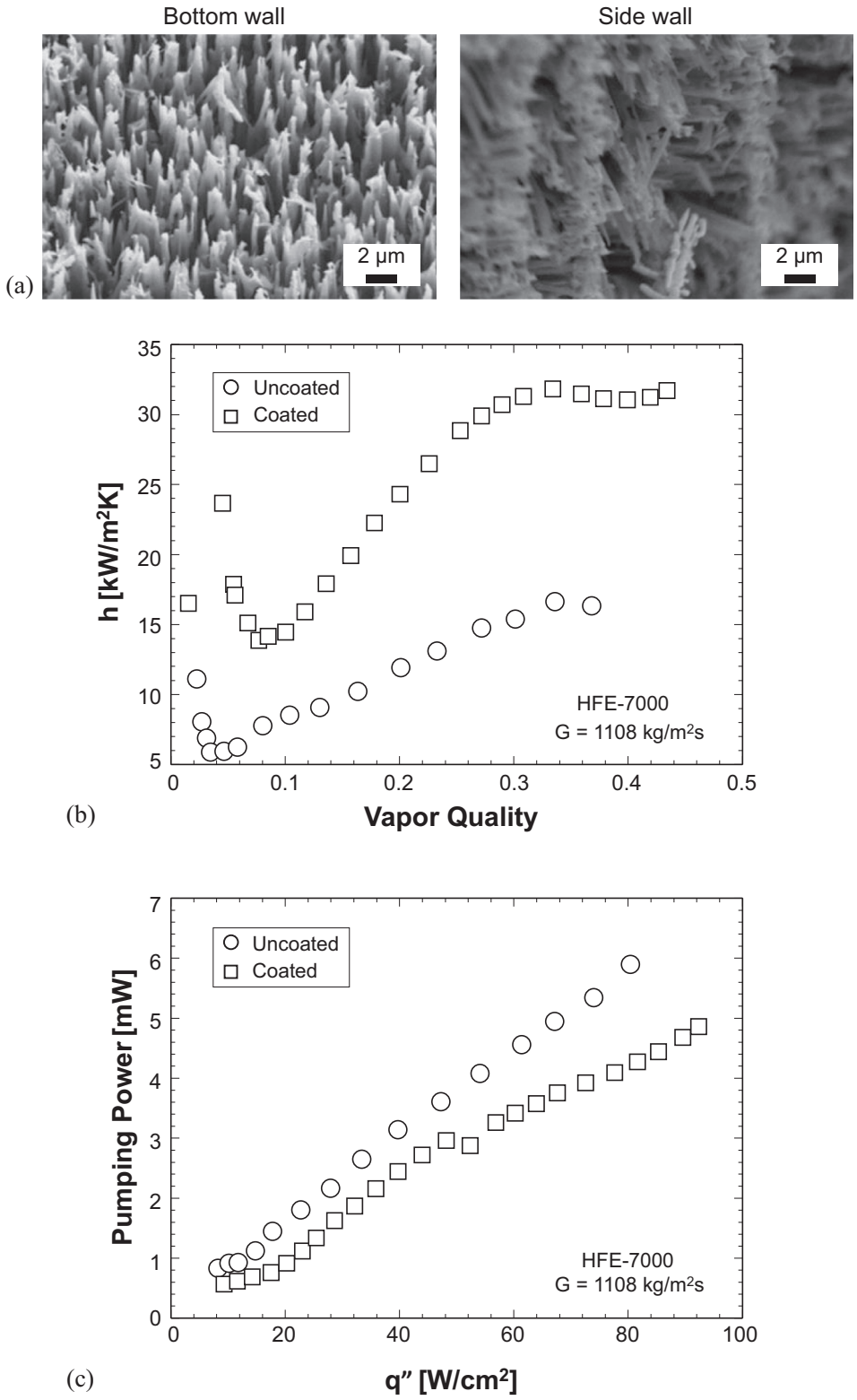

Fig. 10. (a) SEM images of silicon nano-wire coatings. Comparisons of HFE-7000 performance with and without coating at $G = 1108$ kg/m^{2}s for (b) heat transfer coefficient and (c) pumping power. Adapted from Yang et al. [206].

dominant at the liquid-vapor interface for fully-grown bubbles, which helped bubble removal and rewetting. Alam et al. [211] also reported that heat transfer performance of micro-channels with one-sided nanowire coating was insensitive to heated surface orientation, upward- or downward-facing.

However, Shin et al. [212] observed that silicon nanowires in a 8×8-mm^2 channel improved wettability for water but degraded it for FC-72. For water, contact angle decreased from 43.6° for uncoated surface to 4.5° for coating containing 15.7-μm long silicon nanowires, whereas, for FC-72, contact angle increased from

9.8° to 16.1°. Moreover, the contact angle tended to increase slightly with increasing nanowire length. A possible reason surmised by Shin et al. for decreased wettability in FC-72 was suppression of capillary wicking in the coating, which in turn led to a decrease in CHF. In the same study, effects of nanowire length and Reynolds number on flow boiling heat transfer coefficient were highly non-monotonic.

Ghosh et al. [213] devised a facile and self-limiting chemical oxidation technique to fabricate sharp needle-like superhydrophilic CuO nanostructures in rectangular 0.25×0.5-mm^2 micro-channels, and achieved enhancement in flow boiling performance with no appreciable change in pressure drop. Using 'glancing angle' deposition, Demir et al. [214] tested two nanostructured configurations in a 9×33-mm^2 rectangular channel: random 600-nm-long copper nanorod arrays with average diameter of 150 nm, and periodic 600-nm-long copper nanorod structures with 550-nm average diameter. Both provided appreciable but nearly equal enhancement in flow boiling heat transfer coefficient for water.

4.3. Nanoscale deposition

A simple technique to achieving nanoscale deposition is to coat heating surface with nanoparticles using nanofluid pool boiling. Choi et al. [215] performed subcooled water flow boiling experiments on an Fe_3O_4 nanoparticle-deposited wall in a 10.92-mm diameter tube at relatively high mass velocities of 1000–5000 kg/m^{2}s and subcoolings from 20 to 60 °C. They achieved up to 40% CHF enhancement, which they attributed to increased surface wettability, and quantified the effects of nanoparticle deposition using the liquid sublayer dryout model and Kelvin-Helmholtz instability. However, their tests revealed a serious drawback of nanoparticle deposition, as nanoparticles were observed to detach from the surface following CHF occurrence, especially at high mass fluxes, as shown in Fig. 11. Other problematic trends were reported by Ahn et al. [216], who showed that increased surface wettability by Al_2O_3 nanoparticle deposition actually decreased flow boiling heat transfer coefficient for water and delayed boiling inception compared to uncoated surface. Somewhat similar findings were reported by Morshed et al. [217], who measured marginal reductions in water heat transfer coefficient in both the single- and two-phase regions in a 672-μm hydraulic diameter rectangular channel having Al_2O_3 nanoparticle coating, despite some increase in CHF. Morshed et al. also reported that most of the loosely attached nanoparticles were washed away by the flowing liquid, leaving behind only a very thin layer of coating that was able to sustain several flow boiling tests. Ahn et al. [218] explained mechanisms of flow boiling enhancement on nanoparticle-coated surfaces based on the concept of wetting zone fraction.

Overall, there is ample evidence in the published literature that surface treatments consisting of nanoparticle deposition by nanofluid boiling suffer high risk of particle detachment, which poses serious concerns over long-term sustainability of heat transfer performance.

Aside from use of nanofluid boiling to generate nanoscale deposition, other methods have been suggested. Morshed et al. [219] produced a Cu-Al_2O_3 nanocomposite coating on bottom surface of a rectangular 672-μm hydraulic diameter micro-channel using electro co-deposition. Using water as coolant, this coating enhanced water flow boiling heat transfer coefficient by 30–120% and CHF 35–55%, depending on flow rate and wall temperature, with a pressure drop penalty of less than 15%. Additionally, there were no noticeable changes in surface morphology after about 100 h of flow boiling. Meanwhile, Morshed et al. [220] found that the hybrid method combining nanoparticle deposition and micro-grooves in a 5×0.372-mm^2 channel compromised enhancement of water flow boiling heat transfer coefficient compared to a channel with micro-grooves alone.

Liu et al. [221] used liquid phase deposition to form TiO_2 nanometer coating on the inner wall of a 38-mm diameter tube. They achieved enhancement in flow boiling heat transfer coefficient for water and calcium carbonate solution, which they attributed to reduced wettability, and noted absence of fouling after prolonged testing. Kumar et al. [222] devised a porous alumina coating for copper surfaces using spray pyrolysis, and achieved early boiling inception and high nucleation density for water flow

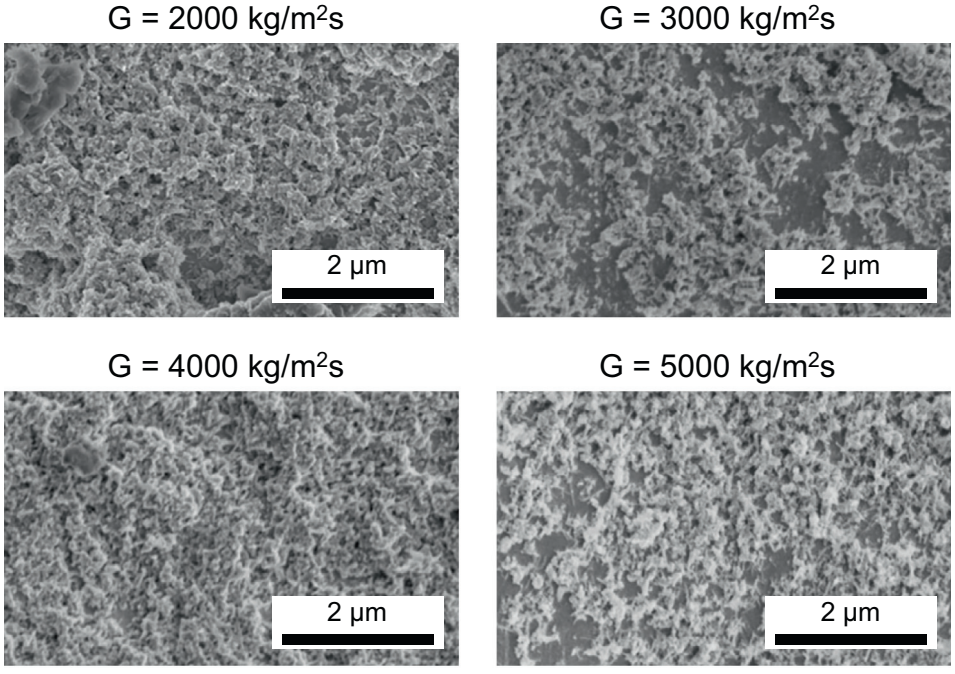

Fig. 11. SEM images of nanoparticle-coated surfaces following water flow boiling. Increasing mass velocity is shown increasing nanoparticle detachment from surface. Adapted from Choi et al. [215].

boiling in a 0.4 × 20-mm^2 rectangular channel. Follow-up work by Kumar et al. [223] included effects of spray pyrolyzed Fe doped Al_2O_3-TiO_2 composite coatings on water flow boiling performance. Using 7.2% Fe doped Al_2O_3-TiO_2 and 88 kg/m^{2}s mass velocity, they achieved enhancements in heat transfer coefficient and CHF as high as 44.11% and 52.39%, respectively. Kumar et al. [224] also used spray pyrolysis aided by surfactant addition to generate ZnO-Al_2O_3 coating, and achieved improvements in both flow boiling heat transfer coefficient and CHF for water.

Çıkım et al. [225] modified inner walls of 249-, 507- and 908-μm diameter tubes with cross-linked pHEMA coatings having thicknesses in the range of 50–150 nm. Using water as coolant, flow boiling heat transfer coefficient and CHF were enhanced by up to 126.2% and 29.7%, respectively; the former was attributed to increases in nucleation site density and incidence of bubbles departing from surface. Overall, thicker pHEMA coatings yielded better enhancements in both heat transfer coefficient and CHF.

Nedaei et al. [226] used initiated chemical vapor deposition to coat pPFDA on inner walls of 889- and 600-μm diameter tubes in thicknesses of 50 to 160 nm. This scheme improved water flow boiling heat transfer coefficient significantly, which was attributed to increased nucleation site density resulting from enhanced hydrophobicity and nanoporous structure. And, here too, thicker coatings led to higher heat transfer coefficients. By using Raman spectroscopy to analyze coated micro-tubes following flow boiling experiments, Nedaei et al. concluded their coatings were both reliable and reproducible.

4.4. Modified surface wettability

Choi et al. [227] studied flow boiling performance in rectangular 505.5- and 508.1-μm hydraulic diameter micro-channels having different surface wettabilities, and used flow visualization to capture dominant mechanisms. They chemically treated a hydrophilic bare photosensitive glass micro-channel to achieve hydrophobic behavior. As shown in Fig. 12(a), boiling heat transfer coefficient for water in the hydrophobic micro-channel was higher than in the hydrophilic, and advantage of the former was attributed to increased nucleation site density and liquid film motion. On the other hand, pressure drop in the hydrophobic micro-channel was higher than that in the hydrophilic, Fig. 12(b), because of unstable motions of bubble and liquid film in the former. Phan et al. [228] achieved similar results for water flow boiling in a 0.5 × 5-mm^2 rectangular channel with exit vapor qualities below 0.1.

In contrast, other investigators suggested that hydrophilicity was more beneficial to flow boiling performance. For example, Zhou et al. [229] investigated impact of contact angle on water flow boiling on bottom surface of a 0.52 × 5.01-mm^2 rectangular micro-channel. Two surfaces were tested: bare hydrophobic silicon wafer having a contact angle of 65°, and superhydrophilic surface having a contact angle of less than 5° that was formed by depositing 100-nm-thick silicon dioxide film using PECVD. Flow visualization showed local dryout occurring on the untreated hydrophilic bare surface at high heat flux and low mass flux, accompanied by overall deterioration in heat transfer performance, trend not observed on the super-hydrophilic surface at identical operating conditions [230]. And, heat transfer deterioration with the bare surface became more severe with increasing inlet vapor quality. On the contrary, the treated superhydrophilic surface overcame these performance drawbacks without incurring increased pressure drop.

Ahmadi and Okawa [231] examined effects of surface wettability on bubble behavior in upward water flow boiling in a 10 × 20-mm^2 rectangular channel. At or close to boiling inception, bubbles on the hydrophobic surface stuck to nucleation sites, growing and contraction at their respective sites, but bubbles on the hydrophilic surface departed immediately from nucleation sites.

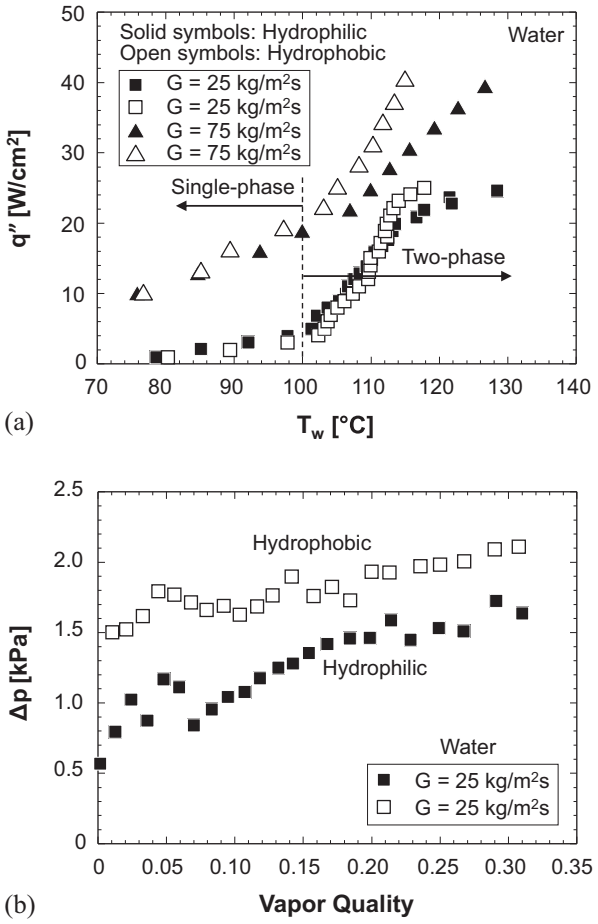

Fig. 12. (a) Boiling curve and (b) pressure drop for water flow boiling in hydrophilic and hydrophobic rectangular micro-channels. Adapted from Choi et al. [227].

Aside from channels with homogenous wettability, a few studies addressed flow boiling heat transfer enhancement for channels with hybrid wettability. Using graphitic petal-decorated CNT coatings synthesized by a two-step microwave plasma enhanced chemical vapor deposition, Kousalya et al. [232] studied water flow boiling in a 5.5-mm high rectangular channel having heterogeneous wetting surfaces with alternating superhydrophobic and superhydrophilic parallel stripes. They showed the heterogeneous surface with high superhydrophilic area fraction greatly reduced surface superheat and enhanced heat transfer coefficient compared to a homogeneous wetting surface. Flow visualization revealed enhanced active nucleation site density and preferential bubble nucleation in the superhydrophobic portions of surface with heterogeneous wettability. Isolated spherical vapor morphologies on surfaces with higher superhydrophilic area fraction promoted thin film evaporation and enhanced bubble ebullition cycle, leading to improved overall two-phase thermal performance.

Kim et al. [233] studied water flow boiling in a 7.5-mm hydraulic diameter rectangular channel having hydrophobic stripes with different widths and directions. They found that CHF for the parallel striped surface was higher than for the cross-striped, and, for both directions, narrow stripes yielded higher CHF. And, differences in flow boiling heat transfer coefficient for the parallel striped surfaces were minor, but considerable for the crossed striped.

Overall, hydrophobicity provides the benefit of earlier boiling incipience but with the disadvantage of lower CHF. On the other hand, hydrophilicity improves nucleate boiling heat transfer and

CHF because of rapid bubble detachment from the surface and enhanced surface rewetting beneath the bubble, albeit at the expense of delayed boiling incipience. This suggests that hybrid-wettability surfaces could combine the advantages of both hydrophobic and hydrophilic surfaces while overcoming their disadvantages, which warrants further study of this form of enhancement.

5. Hybrid multiscale enhancement

As discussed in the previous sections, attempts have been made by several investigators to combine heat transfer merits of different enhancement schemes in pursuit of heat transfer performance superior to those of individual schemes when implemented separately. But these 'hybrid' schemes often involve same enhancement scale.

Another more powerful hybrid enhancement strategy is to combine enhancement schemes incorporating vastly different length scales. Such is the case with a technique developed by Mudawar and Anderson [234] originally for pool boiling situations, which involves combining macro (cm scale) extended surfaces (studs), micro-fins (mm scale), and cavity-promoting (nm scale) surface finish. A typical such surface is formed by first machining the largest stud, then machining micro-studs or micro-grooves along the perimeter of the large stud. Finally, the entire surface is vapor blasted, producing an abundance of small cavities. This multilevel enhancement surface was especially effective at eliminating incipient overshoot and ameliorating pool boiling performance, achieving a 7.5-fold enhancement in CHF for saturated FC-72 and 11.3-fold for subcooled compared to plain surface.

Capitalizing on this attractive performance, Mudawar and co-workers [2] devised a multilevel enhancement surface for channel flow boiling that not only took advantage of the benefits of each scale, but also served to alter fluid flow to greatly increase CHF. As shown in Fig. 13, it consists of an array of large (cm scale) cylindrical studs, which serve to greatly increase heat transfer area, upon each parallel circumferential micro-grooves (mm scale) are formed, contributing further area increase in addition to providing sharp corners highly favorable for bubble nucleation. The entire surface is finally vapor blasted, producing an abundance of μm-scale cavities. Aside from modifying the heat transfer surface itself, this scheme also greatly modified flow structure by creating jet impingement effect upon the front of each stud, followed by routing the flow into circumferential micro-channels between the stud perimeter and preferentially shaped cover plate. This scheme was especially effective at high subcooling, yielding a CHF for water in excess of 1900 W/cm^2.

6. Instabilities and mitigation strategies for flow boiling

6.1. Instability types

As discussed in the previous sections, several investigators have reported various manifestations of instability in channel flow

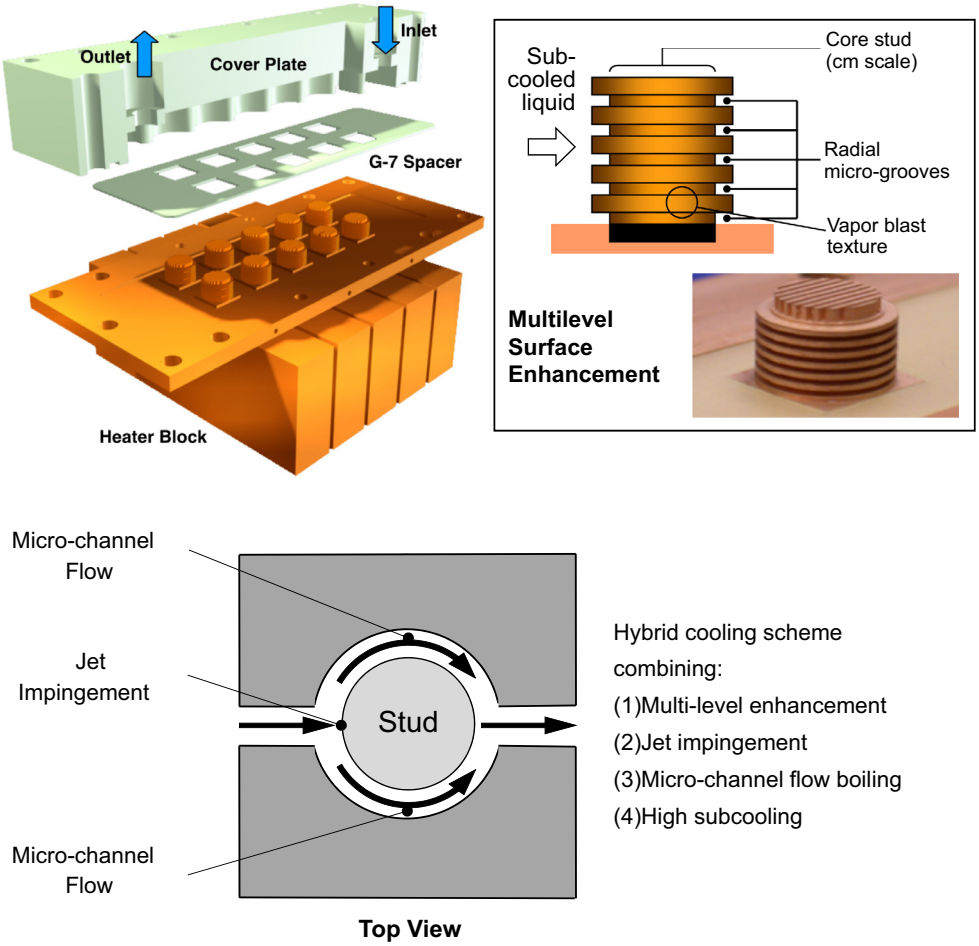

Fig. 13. Hybrid multilevel enhancement scheme for very high flux applications combining cm, mm, and nm enhancement scales, and modifying subcooled channel flow to achieve frontal jet impingement and circumferential micro-channel flow. Adapted from Mudawar [2].

boiling, and suggested that modifying the heat transfer surface and/or flow channel may mitigate some or all instabilities. It is therefore imperative to (1) determine the different types of two-phase flow instabilities, especially for flow in micro-channels, (2) address effectiveness of combined surface and flow channel modification methods at mitigating instabilities, and (3) explore other mitigation methods external to the flow boiling module.

Qu and Mudawar [235] identified two types of two-phase water flow instabilities in a micro-channel test module containing 21 parallel 231 × 713-μm^2 rectangular channels: *severe pressure drop oscillation*, Fig. 14(a), and *mild parallel channel instability*, Fig. 14(b). The former was attributed to interactions between compressible volume within the micro-channel module and that in the two-phase loop external to the test module. This form of instability gained intensity with increasing heat flux, culminating with the two-phase mixture oscillating severely, albeit in unison among parallel micro-channels, between the module's inlet and outlet plenums, eventually penetrating into the upstream plenum and triggering pre-mature CHF. Qu and Mudawar recommended an effective remedy for severe pressure drop oscillation consisting of upstream throttling in order to isolate the test module's compressible volume from that of the external two-phase flow loop. But throttling could not eliminate the second mild parallel channel instability, which consisted of random yet less severe fluctuations that could be tolerated over a broad range of heat fluxes.

Wang and Cheng [236] reported three types of unstable water flow boiling modes in eight parallel trapezoidal 186-μm hydraulic diameter micro-channels: liquid/two-phase alternating flow at low heat flux and high mass velocity, continuous two-phase flow at medium heat flux and medium mass velocity, and liquid/two-phase/vapor alternating flow at high heat flux and low mass velocity. Follow work by Wang et al. [237] identified two unstable water flow boiling regimes in trapezoidal 186-μm hydraulic diameter micro-channels: the first associated with long-period (>1 s) oscillations in temperature and pressure, caused by expansion of vapor bubbles from downstream, and a second with short-period (less than 0.1 s) oscillations, resulting from flow pattern transition from annular to mist. Huh et al. [238] matched periodic fluctuations in wall temperature, pressure drop, and mass velocity for water flow boiling in a heat sink having 103.5-μm hydraulic diameter micro-channels to transition between two alternating flow patterns: bubbly/slug and elongated slug/semi-annular. They also encountered the same vapor flow reversal reported earlier by Qu and Mudawar as shown in Fig. 14(c).

Given the importance of flow stability to phase change cooling applications involving micro-channel heat sinks, several passive methods have been suggested to mitigate instabilities, which can be classified into three categories: upstream throttling, downstream expansion, and auxiliary jetting.

6.2. Upstream throttling

A popular method for eliminating vapor flow reversal and potential for pre-mature CHF is to adopt the tactic of upstream throttling recommended by Qu and Mudawar. This can be achieved either with the aid of a valve situated upstream of the boiling module, or internally at inlets of individual micro-channels.

Wang et al. [239] compared three types of inlet/outlet configurations in pursuit of optimum strategy for instability mitigation for water flow boiling in a heat sink containing parallel 186-μm hydraulic diameter trapezoidal micro-channels. Of the three, one with channel inlet restriction but no outlet restriction showed the least instability. Fig. 15 shows stabilized flow boiling patterns at different mass velocities resulting from this configuration.

Lee et al. [240] achieved instability suppression for water flow boiling in a micro-channel heat sink containing 48 parallel 353-μm hydraulic diameter rectangular micro-channels by installing an orifice at the inlet to each channel or expanding the micro-channels downstream. Odom et al. [241] also adopted upstream orifice throttling to mitigate instabilities for R-134a flow boiling in a heat sink containing an array of 245-μm hydraulic diameter rectangular micro-channels. However, the orifices they used were adjustable, allowing rapid change in upstream resistance to provide sufficient pressure drop to reduce oscillations without having to remove or replace components within the test module.

Sitar et al. [242] used an inlet manifold with gradual reduction of channel cross-section, inlet restrictors, and artificial cavities to stabilize water and FC-72 flow boiling in micro-channel heat sinks having 25- and 50-μm wide square micro-channels. Koşar et al. [243] investigated geometrical effects of inlet orifices on suppression of water flow boiling instabilities in a micro-channel heat sink containing parallel 227-μm hydraulic diameter rectangular micro-channels. Zhang et al. [244] pointed out that use of inlet restriction to suppress instability can greatly increase pressure drop, often beyond capabilities of micro or mini-pumps used in cooling applications. Instead, they built up a framework for transient analysis and active control of micro-channel flow oscillations at the system level, which they validated for water flow boiling in 100-μm hydraulic diameter micro-channels.

6.3. Downstream expansion

Pan and co-workers [245,246] proposed that, unlike micro-channel heat sinks having uniform flow channels, Fig. 16(a), use of diverging channels, Fig. 16(b), may help improve flow boiling stability. They confirmed effectiveness of this strategy for water flow boiling in 33.3 and 120-μm hydraulic diameter channels with diverging angles of 0.183° and 0.5°, respectively. Follow-up work by Lu and Pan [247,248] and Fu et al. [249] combined use of diverging parallel micro-channels with different distributions of laser-etched artificial nucleation sites to further improve flow boiling stability.

Balasubramanian et al. [250] devised a different method to achieving downstream flow expansion in micro-channel heat sinks consisting of removal of downstream fins. They demonstrated effectiveness of this approach by improved flow stability for water, evidenced by improved heat transfer performance coupled with reduced wall temperature and pressure drop fluctuations. In follow-up work, Balasubramanian et al. [25] proposed using micro-channels having stepped fins (with fins height decreasing 400 μm per step) to reduce water flow boiling instabilities in straight channels. Using numerical methods and water as working fluid, Hardt et al. [251] proposed modifying 100-μm wide micro-channels with asymmetric surface features consisting of periodic, triangular-shaped indentations to promote unidirectional bubble growth in pursuit of better flow stability. This technique was based on merits of capillary force and pinning/de-pinning of three-phase contact lines at sharp edges of wall geometry.

Hong et al. [252] proposed a parallelogram configuration, Fig. 16(c), of ultra-shallow micro-channels with aspect ratio of 5 to replace the rectangular configuration, Fig. 16(a). The goal here was to suppress acetone flow instabilities by relieving upstream vapor blockage and accelerating bubble movement toward the outlet, thereby maintaining steady fluid supply to the channels. Prajapati et al. [253] compared boiling performances of water flow boiling in parallel 522-μm channels using three different configurations: uniform cross-section, diverging cross-section, and segmented fin micro-channels. They showed that the segmented fin channels with interconnected flow passage provided the most superior heat transfer performance with pressure drop comparable to those of the other two configurations. In terms of flow boiling instability, bubble clogging and flow reversal were worst in

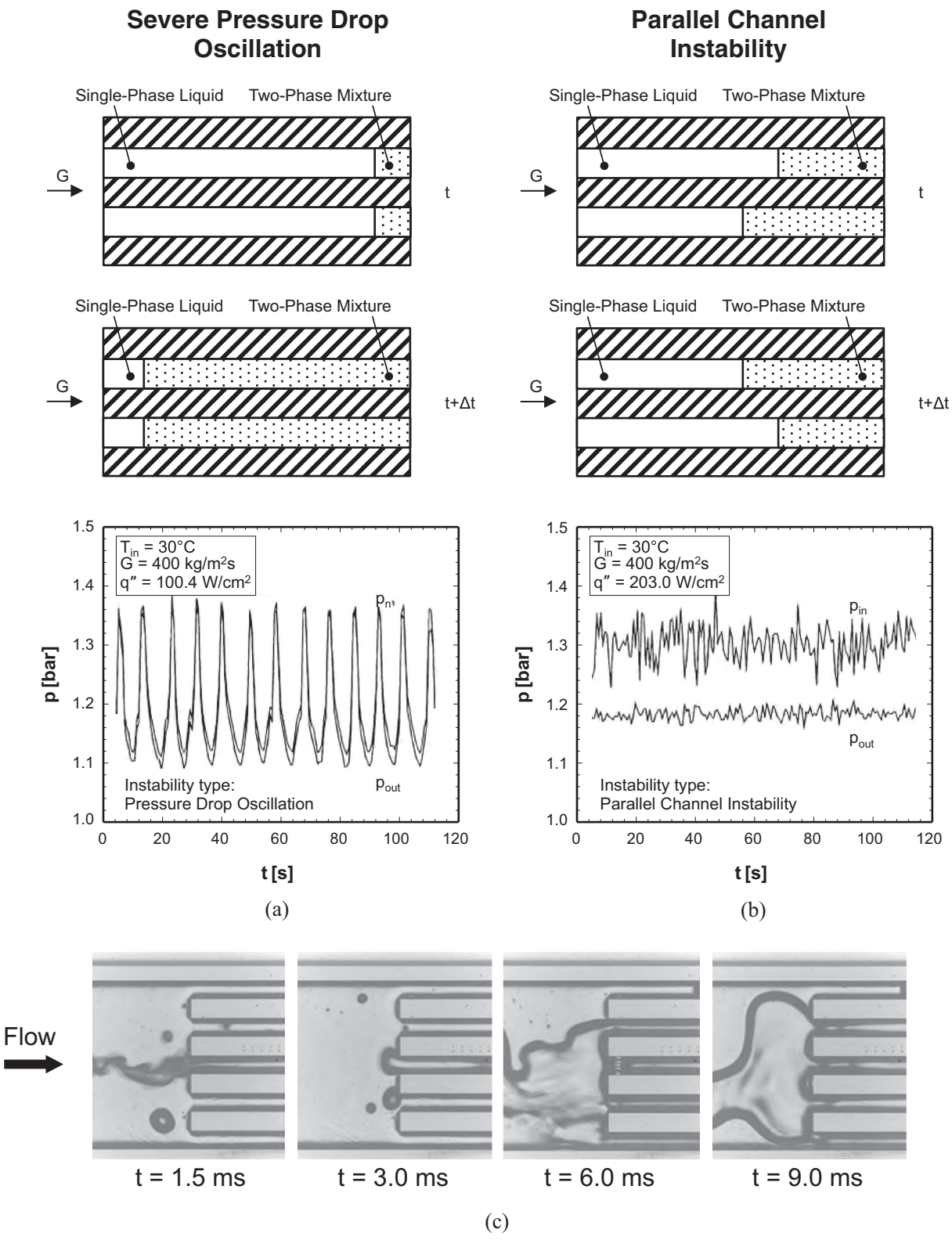

Fig. 14. Temporal records of inlet and outlet pressures during (a) severe pressure drop oscillation and (b) mild parallel channel instability (adapted from Qu and Mudawar [235]). (c) Flow reversal into upstream plenum (adapted from Koşar et al. [243]).

uniform cross-section channels, and could be partially resolved with diverging channels. Overall, the segmented channels relieved the problem of bubble clogging, allowing smooth and easy passage of growing bubbles, as well as eliminating flow reversal.

Miner et al. [254] performed numerical study of flow boiling in micro-channels with expanding cross-sectional area resulting from increasing channel depth. Their model predicted that water CHF values exceeding 600 W/cm^2 were possible with sufficient

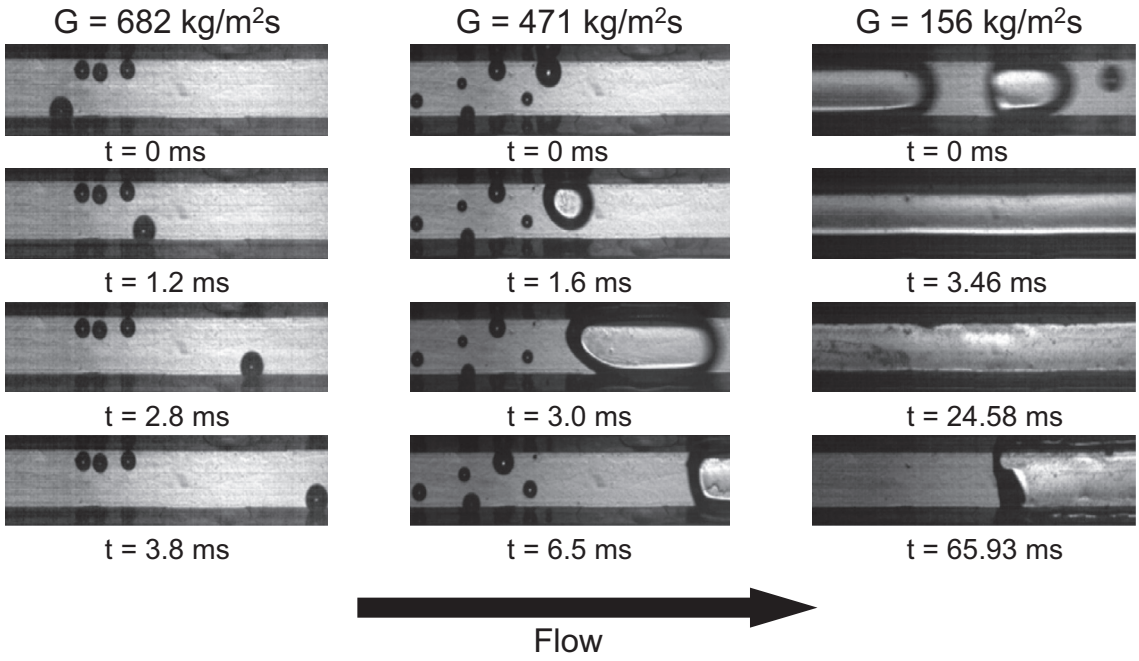

Fig. 15. Images of stable water flow boiling patterns near outlet of parallel trapezoidal micro-channels, achieved with inlet restriction but no outlet restriction, corresponding to three mass velocities at q'' = 36.5 W/cm^2 and T_{in} = 35 °C. Adapted from Wang et al. [239].

expansion of channel width and height. In follow-up study, Miner et al. [255,256] experimentally investigated R-134a flow boiling in micro-channels featuring base expansion, defined relative to base expansion angle. They found that increasing expansion angle reduced pressure drop, resisted heater dryout, and delayed CHF. Miner and Phelan also [257] assessed several correlations and models for enhanced flow boiling CHF via cross-sectional expansion.

6.4. Auxiliary jetting flow

The concept of hybrid micro-channel/jet-impingement cooling was proposed and explored extensively by Sung and Mudawar for both single-phase and two-phase applications [2,23,258–260] using circular and rectangular jets issued into individual channels. While two-phase micro-channels alone offer several important advantages, such as small size and weight, minimal coolant inventory, and high convective heat transfer coefficient, they can produce high pressure drop and appreciable temperature gradients along the direction of coolant flow when dissipating very high heat fluxes. On the other hand, jet impingement is known to produce high heat transfer coefficients in the impingement zone and require smaller pressure drop than micro-channels, but they can produce relatively large surface temperature gradients away from the impingement zone. Use of multiple impinging jets can diffuse temperature gradients over large surface areas, but this both greatly increases coolant flow rate and complicates routing of spent coolant between impingement zones. Overall, the hybrid micro-channel/jet-impingement cooling scheme was devised to combine the performance merits of the individual schemes while eliminating most of their shortcomings. In fact, this hybrid scheme achieved heat fluxes as high as 1127 W/cm^2 [258–260] corresponding to stable flow and low vapor void fraction using HFE-7100, which is known for having relatively poor thermophysical properties.

Yang et al. [261,262] proposed a rather similar method to enhance water flow boiling stability in a micro-channel heat sink having parallel 200 × 250-μm^2 channels. Connected to each main channel were two 50 × 250-μm^2 channels that introduced auxiliary liquid to hasten bubble collapse by condensation. They concluded that this structure was self-sustaining, and provided both flow stability and improved heat transfer, aided by strong mixing from high frequency collapse of elongated bubbles in the main channels. Li et al. [263,264] further developed this scheme for HFE-7100 using multiple auxiliary 60 × 250-μm^2 channels to supply liquid to each 200 × 250-μm^2 main channel. They indicated that the auxiliary supply junctions acted as micro-nozzles that disrupted formation of elongated bubbles in the main channels as suggested earlier by Sung and Mudawar. Recently, Li et al. [265,266] combined use of multiple auxiliary channels (micro-nozzles) with micro-scale reentrant cavities (30-μm diameter and 6-μm opening) in the main channel walls to enhance flow boiling. The multiple jets helped maintain continuous rewetting, while the cavities supported formation of a thin liquid film on sidewalls. Using water as coolant, they achieved CHF values in excess of 1000 W/cm^2 with 50% less mass velocity than Yang et al.'s two-nozzle configuration, and 55% reduction in pressure drop.

Dai et al. [267] adopted a flow separation technique that routed a portion of the inlet flow through a micro-jet that injected liquid into the main 5.5-mm wide and 0.34-mm high channel, as shown in Fig. 17. This technique both enhanced water flow boiling heat transfer coefficient and reduced pressure drop. They attributed these performance merits to ability of the micro-jet to suppress bubble growth in the main channel, and reported observable suppression of flow instabilities. Vutha et al. [268] devised an active technique to enhance flow boiling stability involving supply of ambient temperature liquid into the main 210-μm high micro-channel.

6.5. Vapor venting

Instead of injecting liquid, venting vapor from micro-channels is another technique that has been proposed to suppress instabilities. Earlier works by Meng et al. [269,270] involved venting of dis-

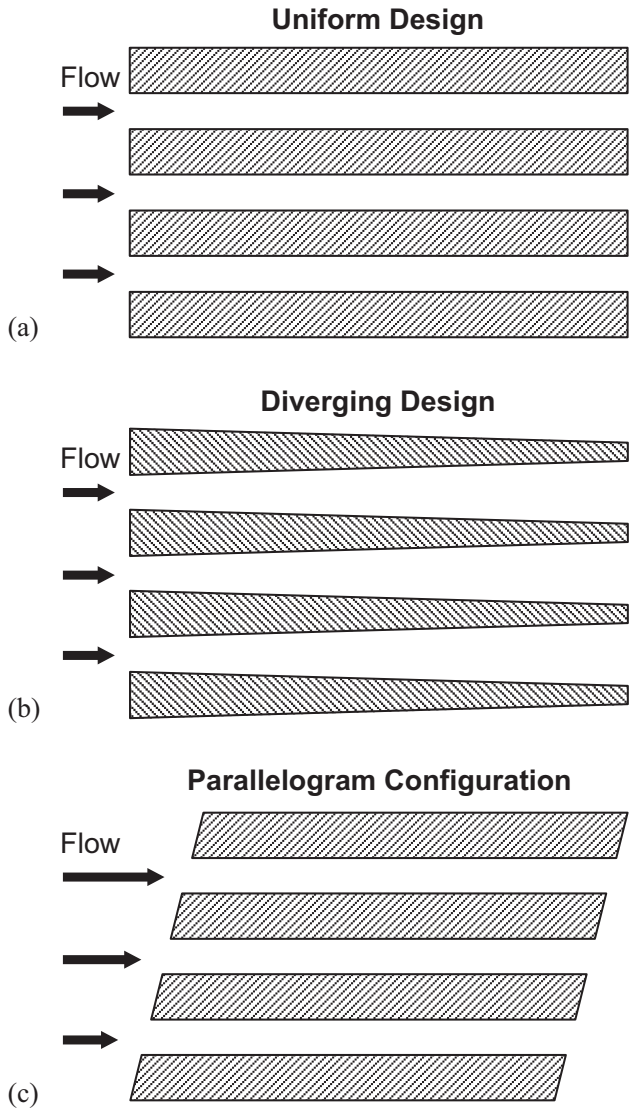

Fig. 16. Schematics of micro-channels with (a) uniform cross-section, (b) diverging cross-section, and (c) parallelogram configuration.

solved gas from water and methanol using a nanoscale porous polypropylene membrane to reduce pressure drop and improve reaction in Direct Methanol Fuel Cells. Regarding flow boiling in micro-channels, David and his co-workers [271–273] proposed to locally vent vapor produced in 98×124-μm^2 micro-channels through a 65-μm thick hydrophobic Teflon membrane, featuring 220-nm diameter pores, which capped the channels. Pressure drop was up to 60% lower with venting than without, and this reduction was deemed potentially beneficial to mitigating detrimental flow instabilities.

6.6. Other methods for instability suppression

Xu et al. [274] and Liu et al. [275] proposed using seed bubbles generated by micro-heaters located in the upstream region of micro-channels to stabilize flow boiling of acetone and methanol in a heat sink having parallel 100-μm hydraulic diameter rectangular channels. Low-frequency (10 Hz) seed bubbles not only decreased oscillation amplitudes of pressure drop, inlet and outlet temperatures, and wall temperature, but also shortened oscillation cycle period. On the other hand, high-frequency (100 Hz or higher) seed bubbles suppressed flow instabilities altogether. Bhide et al.

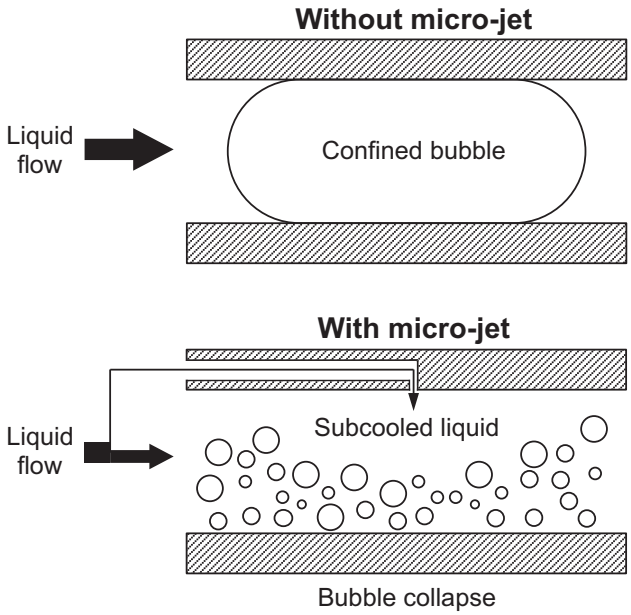

Fig. 17. Mechanism of micro-jet injection into main channel to enhance boiling heat transfer, reduce pressure drop, and suppress flow instabilities.

[276] proposed applying external pulsations to flow in a 136.8-μm hydraulic diameter trapezoidal micro-channel to reduce pressure oscillations.

Han and Shikazono [277] used air injection to stabilize wall temperature and inlet/outlet pressures for water flow boiling in a 0.5-mm diameter tube. A similar concept was also adopted by Liu et al. [278]. However, this technique causes significant changes to two-phase flow structure and heat transfer performance. Additionally, inclusion of non-condensable gas can greatly compromise heat transfer performance of the flow loop's condenser.

Liu et al. [279] evaluated different approaches to mitigating water flow boiling instabilities in 0.105×1-mm^2, 30-mm long micro-channels. Their tests featured three different channel surface wettabilities: hydrophilic (having water contact angle of 36°), formed by plasma etching, hydrophobic (103°), achieved by application of thin coating of low surface energy material, and superhydrophilic (near 0°), formed by growing nanowire arrays. They reported that the hydrophobic and superhydrophilic surfaces were both free from temperatures oscillations. Xu et al. [280] proposed separating adjacent 75×164-μm^2 rectangular micro-channels with a wall comprised of arrays of 15×15-μm^2 micro fins. Vapor generated from the wall was observed to flow towards the bare channels by surface tension. Xu et al. showed that this method was highly effective at maintaining wall temperature stability for acetone, evidenced by oscillation amplitude of merely 0.02–0.18 °C.

Kuo and Peles [281] reported that reentrant cavities formed inside rectangular 200×253-μm^2 channel walls could help suppress instabilities resulting from rapid vapor bubble growth. Follow-up study by Kuo and Peles [282] showed that boiling instabilities can be significantly delayed at high pressures.

Aside from the above methods of surface modification, increasing inlet subcooling is another means for mitigating instabilities in flow boiling. This advantage and ability to improve flow boiling heat transfer, which have both been demonstrated in many prior studies, are realized by aiding high frequency collapse of large vapor bubbles.

Overall, research addressing mitigation or complete suppression of flow boiling instabilities is still ongoing given the importance of flow stability to a large number of applications involving use of micro-channel heat sinks.

7. Concluding remarks

This article reviewed published literature addressing enhancement of channel flow boiling heat transfer by surface modifications, including macro, micro, nano, and hybrid multiscale methodologies. Also included are various techniques for suppressing flow boiling instabilities, especially in micro-channel heat sinks. Key observations from this review can be summarized as follows:

(1) Macroscale enhancing techniques include cylindrical pins, macro ribs, and twisted tape inserts, which are all effective at improving flow boiling heat transfer coefficient and CHF by increasing heat transfer area and improving vapour-liquid mixing, albeit at the expense of higher pressure drop.
(2) Microscale enhancing techniques include micro-fins, micro-pin-fins, artificial cavities, porous coating, and foam. Key objectives with these methods are to increase nucleation site density during nucleate boiling dominant operation, and improve liquid film stability during convective dominant operation. However, enhanced heat transfer performance is often compromised by greatly increased pressure drop. Additionally, there are cost concerns when implementing certain microscale techniques, especially those involving fabrication of miniature fins. Further study is needed to optimize key parameters for each technique, such size, shape, and layout of micro-fins, shape and size of artificial cavities, and void size in coatings and foams.
(3) Nanoscale enhancing techniques include coating heating surface with nanotubes or nanowires, nanoparticle deposition, or use of hybrid wettability schemes. Key to improving flow boiling heat transfer performance with these techniques is capillary wicking within nanostructures. However, there are contradictory findings surrounding effects of hydrophilicity and hydrophobicity on boiling performance. Unlike macroscale and microscale enhancement features, nanostructure topographies are prone to severe degradation after prolonged boiling. This degradation can take the form of deformation of nanotubes, blockage of nanoscale pores, or gradual detachment of nanostructures from the heating surface.
(4) Multiscale enhancement, combining merits of (a) relatively large (cm scale) studs, to greatly increase heat transfer area, (b) micro-grooves (mm scale), to further increase surface area and provide sharp corners favorable to bubble nucleation, and (c) nucleation promoting cavities, is a very effective means for enhancing flow boiling heat transfer performance. With added ability to favorably alter fluid flow pattern, this scheme has achieved CHF for water in excess of 1900 W/cm^2.
(5) Several techniques have been proposed to suppress instabilities in channel flow boiling, including upstream fluid throttling, downstream fluid expansion, auxiliary jetting, vapor venting, and upstream seed bubble generation. Jet injection into main channels of a micro-channel heat sink has been proven highly effective at both mitigating instabilities and greatly enhancing boiling performance, evidenced by stable heat flux values for HFE-7100 as high as 1127 W/cm^2. Overall, channel flow boiling instabilities are a major practical concern in cooling system design.
(6) Perhaps the most serious obstacle to adopting enhanced surfaces is absence of generalized predictive design tools for different channel shapes and sizes, and different fluids and operating conditions, such as the universal correlations available for two-phase flow and heat transfer in micro-channel heat sinks [283,284]. Additionally, performance prediction will require increased reliance on robust computational models [285] for specific enhancement schemes.

Declaration of Competing Interest

The authors declared that there is no conflict of interest.

Acknowledgements

Support of the National Natural Science Foundation of China under Grant No. 51876025 and the Fundamental Research Funds for the Central Universities under Grant No. DUT19JC10 is gratefully acknowledged.

Appendix A. Supplementary material

Supplementary data to this article can be found online at https://doi.org/10.1016/j.ijheatmasstransfer.2019.118864.

References

[1] T.M. Anderson, I. Mudawar, Microelectronic cooling by enhanced pool boiling of a dielectric fluorocarbon liquid, J. Heat Transfer 111 (1989) 752–759.
[2] I. Mudawar, Recent advances in high-flux, two-phase thermal management, J. Therm. Sci. Eng. Appl. 5 (2013) 021012.
[3] J. Lee, I. Mudawar, Low-temperature two-phase microchannel cooling for high-heat-flux thermal management of defense electronics, IEEE Trans. Compon. Packag. Technol. 32 (2009) 453–465.
[4] I. Mudawar, Assessment of high-heat-flux thermal management schemes, IEEE Trans. Compon. Packag. Technol. 24 (2001) 122–141.
[5] T.J. LaClair, I. Mudawar, Thermal transients in a capillary evaporator prior to the initiation of boiling, Int. J. Heat Mass Transfer 43 (2000) 3937–3952.
[6] I. Mudawar, T.M. Anderson, Parametric investigation into the effects of pressure, subcooling, surface augmentation and choice of coolant on pool boiling in the design of cooling systems for high-power-density electronic chips, J. Electron. Packag. 112 (1990) 375–382.
[7] J.A. Shmerler, I. Mudawar, Local heat transfer coefficient in wavy free-falling turbulent liquid films undergoing uniform sensible heating, Int. J. Heat Mass Transfer 31 (1988) 67–77.
[8] D.E. Maddox, I. Mudawar, Single-and two-phase convective heat transfer from smooth and enhanced microelectronic heat sources in a rectangular channel, J. Heat Transfer 101 (1989) 1045–1052.
[9] T.C. Willingham, I. Mudawar, Forced-convection boiling and critical heat flux from a linear array of discrete heat sources, Int. J. Heat Mass Transfer 35 (1992) 2879–2890.
[10] C.O. Gersey, I. Mudawar, Effects of heater length and orientation on the trigger mechanism for near-saturated flow boiling critical heat flux—I. Photographic study and statistical characterization of the near-wall interfacial features, Int. J. Heat Mass Transfer 38 (1995) 629–641.
[11] J.C. Sturgis, I. Mudawar, Critical heat flux in a long, rectangular channel subjected to one-sided heating—I. flow visualization, Int. J. Heat Mass Transfer 42 (1999) 1835–1847.
[12] J.C. Sturgis, I. Mudawar, Critical heat flux in a long, rectangular channel subjected to one-sided heating—II. Analysis of critical heat flux data, Int. J. Heat Mass Transfer 42 (1999) 1849–1862.
[13] J. Lee, I. Mudawar, Critical heat flux for subcooled flow boiling in micro-channel heat sinks, Int. J. Heat Mass Transfer 52 (2009) 3341–3352.
[14] J. Lee, I. Mudawar, Fluid flow and heat transfer characteristics of low temperature two-phase micro-channel heat sinks–Part 1: experimental methods and flow visualization results, Int. J. Heat Mass Transfer 51 (2008) 4315–4326.
[15] D.D. Hall, I. Mudawar, Ultra-high critical heat flux (CHF) for subcooled water flow boiling—II: high-CHF database and design equations, Int. J. Heat Mass Transfer 42 (1999) 1429–1456.
[16] S. Mukherjee, I. Mudawar, Pumpless loop for narrow channel and micro-channel boiling, J. Electron. Packag. 125 (2003) 431–441.
[17] S. Mukherjee, I. Mudawar, Smart pumpless loop for micro-channel electronic cooling using flat and enhanced surfaces, IEEE Trans. Compon. Packag. Technol. 26 (2003) 99–109.
[18] M.E. Johns, I. Mudawar, An ultra-high power two-phase jet-impingement avionic clamshell module, J. Electron. Packag. 118 (1996) 264–270.
[19] W.P. Klinzing, J.C. Rozzi, I. Mudawar, Film and transition boiling correlations for quenching of hot surfaces with water sprays, J. Heat. Treat. 9 (1992) 91–103.

[20] D.D. Hall, I. Mudawar, Experimental and numerical study of quenching complex-shaped metallic alloys with multiple, overlapping sprays, Int. J. Heat Mass Transfer 38 (1995) 1201–1216.
[21] J.D. Bernardin, I. Mudawar, A cavity activation and bubble growth model of the Leidenfrost point, J. Heat Transfer 124 (2002) 864–874.
[22] M. Visaria, I. Mudawar, Application of two-phase spray cooling for thermal management of electronic devices, IEEE Trans. Compon. Packag. Technol. 32 (2009) 784–793.
[23] M.K. Sung, I. Mudawar, Single-phase hybrid micro-channel/micro-jet impingement cooling, Int. J. Heat Mass Transfer 51 (2008) 4342–4352.
[24] I. Mudawar, D.E. Maddox, Enhancement of critical heat flux from high power microelectronic heat sources in a flow channel, J. Electron. Packag. 112 (1990) 241–248.
[25] K. Balasubramanian, P.S. Lee, C.J. Teo, S.K. Chou, Flow boiling heat transfer and pressure drop in stepped fin microchannels, Int. J. Heat Mass Transfer 67 (2013) 234–252.
[26] I. Mudawar, M.B. Bowers, Ultra-high critical heat flux (CHF) for subcooled water flow boiling—I: CHF data and parametric effects for small diameter tubes, Int. J. Heat Mass Transfer 42 (1999) 1405–1428.
[27] P.A. Kew, K. Cornwell, Correlations for the prediction of boiling heat transfer in small-diameter channels, Appl. Therm. Eng. 17 (1997) 705–715.
[28] C.L. Ong, J.R. Thome, Macro-to-microchannel transition in two-phase flow: Part 1 – Two-phase flow patterns and film thickness measurements, Exp. Therm. Fluid Sci. 35 (2011) 37–47.
[29] S.S. Mehendale, A.M. Jacobi, R.K. Shah, Fluid flow and heat transfer at micro- and meso-scales with application to heat exchanger design, Appl. Mech. Rev. 53 (2000) 175–193.
[30] P. Cheng, H.-Y. Wu, F.-J. Hong, Phase-change heat transfer in microsystems, J. Heat Transfer 129 (2006) 101–108.
[31] A.E. Bergles, R.L. Webb, G.H. Junkhan, M.K. Jensen, Bibliography on augmentation of convective heat and mass transfer, Heat Transfer Laboratory Report HTL-19, Iowa State University, 1979.
[32] H. Zhang, I. Mudawar, M.M. Hasan, Experimental assessment of the effects of body force, surface tension force, and inertia on flow boiling CHF, Int. J. Heat Mass Transfer 45 (2002) 4079–4095.
[33] H. Zhang, I. Mudawar, M.M. Hasan, Flow boiling CHF in microgravity, Int. J. Heat Mass Transfer 48 (2005) 3107–3118.
[34] C. Konishi, I. Mudawar, Review of flow boiling and critical heat flux in microgravity, Int. J. Heat Mass Transfer 80 (2015) 469–493.
[35] I. Mudawar, Flow boiling and flow condensation in reduced gravity, Adv. Heat Transfer 49 (2017) 225–306.
[36] R.L. Webb, G.H. Junkhan, A.E. Bergles, Bibliography of US patents on augmentation of convective heat and mass transfer, Heat Transfer Laboratory Report HTL-25, Iowa State University, 1980.
[37] Z. Wu, B. Sundén, On further enhancement of single-phase and flow boiling heat transfer in micro/minichannels, Renewable Sustainable Energy Rev. 40 (2014) 11–27.
[38] K.C. Leong, J.Y. Ho, K.K. Wong, A critical review of pool and flow boiling heat transfer of dielectric fluids on enhanced surfaces, Appl. Therm. Eng. 112 (2017) 999–1019.
[39] M. Shojaeian, A. Koşar, Pool boiling and flow boiling on micro-and nanostructured surfaces, Exp. Therm. Fluid Sci. 63 (2015) 45–73.
[40] M. McCarthy, K. Gerasopoulos, S.C. Maroo, A.J. Hart, Materials, fabrication, and manufacturing of micro/nanostructured surfaces for phase-change heat transfer enhancement, Nanoscale Microscale Thermophys. Eng. 18 (2014) 288–310.
[41] D.E. Kim, D.I. Yu, D.W. Jerng, M.H. Kim, H.S. Ahn, Review of boiling heat transfer enhancement on micro/nanostructured surfaces, Exp. Therm. Fluid Sci. 66 (2015) 173–196.
[42] D. Attinger, C. Frankiewicz, A.R. Betz, T.M. Schutzius, R. Ganguly, A. Das, C.-J. Kim, C.M. Megaridis, Surface engineering for phase change heat transfer: a review, MRS Energy Sustainability 1 (2014) E4.
[43] D.P. Shatto, G.P. Peterson, A review of flow boiling heat transfer with twisted tape inserts, J. Enhanced Heat Transfer 3 (1996) 233–257.
[44] Y.K. Prajapati, P. Bhandari, Flow boiling instabilities in microchannels and their promising solutions – A review, Exp. Therm. Fluid Sci. 88 (2017) 576–593.
[45] G. Liang, I. Mudawar, Review of mass and momentum interactions during drop impact on a liquid film, Int. J. Heat Mass Transfer 101 (2016) 577–599.
[46] G. Liang, I. Mudawar, Review of drop impact on heated walls, Int. J. Heat Mass Transfer 106 (2017) 103–126.
[47] G. Liang, I. Mudawar, Review of spray cooling–Part 1: single-phase and nucleate boiling regimes, and critical heat flux, Int. J. Heat Mass Transfer 115 (2017) 1174–1205.
[48] G. Liang, I. Mudawar, Review of spray cooling–Part 2: high temperature boiling regimes and quenching applications, Int. J. Heat Mass Transfer 115 (2017) 1206–1222.
[49] G. Liang, I. Mudawar, Pool boiling critical heat flux (CHF)–Part 1: review of mechanisms, models, and correlations, Int. J. Heat Mass Transfer 117 (2018) 1352–1367.
[50] G. Liang, I. Mudawar, Pool boiling critical heat flux (CHF)–Part 2: assessment of models and correlations, Int. J. Heat Mass Transfer 117 (2018) 1368–1383.
[51] G. Liang, I. Mudawar, Review of pool boiling enhancement with additives and nanofluids, Int. J. Heat Mass Transfer 124 (2018) 423–453.
[52] G. Liang, I. Mudawar, Review of pool boiling enhancement by surface modification, Int. J. Heat Mass Transfer 128 (2019) 892–933.
[53] G. Liang, I. Mudawar, Review of single-phase and two-phase nanofluid heat transfer in macro-channels and micro-channels, Int. J. Heat Mass Transfer 136 (2019) 324–354.
[54] K.W. Haley, J.W. Westwater, Boiling heat transfer from single fins, in: Proceeding of the 3rd International Heat Transfer Conference, Chicago, USA, 1966, pp. 245–258.
[55] G.J. Klein, J.W. Westwater, Heat transfer from multiple spines to boiling liquids, AIChE J. 17 (1971) 1050–1056.
[56] I. Mudawar, D.E. Maddox, Critical heat flux in subcooled flow boiling of fluorocarbon liquid on a simulated electronic chip in a vertical rectangular channel, Int. J. Heat Mass Transfer 32 (1989) 379–394.
[57] C.H. Kim, I.C. Bang, S.H. Chang, Critical heat flux performance for flow boiling of R-134a in vertical uniformly heated smooth tube and rifled tubes, Int. J. Heat Mass Transfer 48 (2005) 2868–2877.
[58] L. Cheng, G. Xia, Experimental study of CHF in a vertical spirally internally ribbed tube under the condition of high pressures, Int. J. Therm. Sci. 41 (2002) 396–400.
[59] L. Cheng, T. Chen, Flow boiling heat transfer in a vertical spirally internally ribbed tube, Heat Mass Transfer 37 (2001) 229–236.
[60] B. Kim, B. Sohn, An experimental study of flow boiling in a rectangular channel with offset strip fins, Int. J. Heat Fluid Flow 27 (2006) 514–521.
[61] R.S. Reid, M.B. Pate, A.E. Bergles, A comparison of augmentation techniques during in-tube evaporation of R-113, J. Heat Transfer 113 (1991) 451–458.
[62] M.A. Akhavan-Behabadi, R. Kumar, M. Jamali, Investigation on heat transfer and pressure drop during swirl flow boiling of R-134a in a horizontal tube, Int. J. Heat Mass Transfer 52 (2009) 1918–1927.
[63] M.A. Akhavan-Behabadi, R. Kumar, A. Mohammadpour, M. Jamali-Asthiani, Effect of twisted tape insert on heat transfer and pressure drop in horizontal evaporators for the flow of R-134a, Int. J. Refrig. 32 (2009) 922–930.
[64] F.T. Kanizawa, G. Ribatski, Two-phase flow patterns and pressure drop inside horizontal tubes containing twisted-tape inserts, Int. J. Multiphase Flow 47 (2012) 50–65.
[65] F.T. Kanizawa, T.S. Mogaji, G. Ribatski, Evaluation of the heat transfer enhancement and pressure drop penalty during flow boiling inside tubes containing twisted tape insert, Appl. Therm. Eng. 70 (2014) 328–340.
[66] F.T. Kanizawa, T.S. Mogaji, G. Ribatski, A new model for flow boiling heat transfer coefficient inside horizontal tubes with twisted-tape inserts, Int. J. Refrig. 61 (2016) 55–68.
[67] K.N. Agrawal, H.K. Varma, S. Lal, Heat transfer during forced convection boiling of R-12 under swirl flow, J. Heat Transfer 108 (1986) 567–573.
[68] K.N. Agrawal, H.K. Varma, S. Lal, Pressure drop during forced convection boiling of R-12 under swirl flow, J. Heat Transfer 104 (1982) 758–762.
[69] M.K. Jensen, H.P. Bensler, Saturated forced-convective boiling heat transfer with twisted-tape inserts, J. Heat Transfer 108 (1986) 93–99.
[70] J. Yan, Q. Bi, G. Zhu, L. Cai, Q. Yuan, H. Lv, Critical heat flux of highly subcooled water flow boiling in circular tubes with and without internal twisted tapes under high mass fluxes, Int. J. Heat Mass Transfer 95 (2016) 606–619.
[71] T.S. Mogaji, F.T. Kanizawa, E.P. Bandarra Filho, G. Ribatski, Experimental study of the effect of twisted-tape inserts on flow boiling heat transfer enhancement and pressure drop penalty, Int. J. Refrig. 36 (2013) 504–515.
[72] F. Inasaka, H. Nariai, Evaluation of subcooled critical heat flux correlations for tubes with and without internal twisted tapes, Nucl. Eng. Des. 163 (1996) 225–239.
[73] T.W. Arment, N.E. Todreas, A.E. Bergles, Critical heat flux and pressure drop for tubes containing multiple short-length twisted-tape swirl promoters, Nucl. Eng. Des. 257 (2013) 1–11.
[74] H. Nariai, F. Inasaka, Critical heat flux of subcooled flow boiling in tubes with internal twisted tapes, in: Nuclear Thermal Hydraulics Conference, San Francisco, USA, 1991.
[75] V.V. Yagov, Heat transfer and crisis in swirl flow boiling, Exp. Therm. Fluid Sci. 29 (2005) 871–883.
[76] R. Yun, J.-S. Hwang, J.T. Chung, Y. Kim, Flow boiling heat transfer characteristics of nitrogen in plain and wire coil inserted tubes, Int. J. Heat Mass Transfer 50 (2007) 2339–2345.
[77] W. Tong, A.E. Bergles, M.K. Jensen, Critical heat flux and pressure drop of subcooled flow boiling in small-diameter tubes with twisted-tape inserts, J. Enhanced Heat Transfer 3 (1996) 95–108.
[78] H. Kinoshita, T. Yoshida, H. Nariai, F. Inasaka, Study on the mechanism of critical heat flux enhancement for subcooled flow boiling in a tube with internal twisted tape under nonuniform heating conditions, Heat Transfer Jpn. Res. 25 (1996) 293–307.
[79] E.P.B. Filho, J.M.S. Jabardo, P.E.L. Barbieri, Convective boiling pressure drop of refrigerant R-134a in horizontal smooth and microfin tubes, Int. J. Refrig. 27 (2004) 895–903.
[80] E.P.B. Filho, J.M.S. Jabardo, Convective boiling performance of refrigerant R-134a in herringbone and microfin copper tubes, Int. J. Refrig. 29 (2006) 81–91.
[81] S. Wellsandt, L. Vamling, Prediction method for flow boiling heat transfer in a herringbone microfin tube, Int. J. Refrig. 28 (2005) 912–920.
[82] E.P.B. Filho, P.E.L. Barbieri, Flow boiling performance in horizontal microfinned copper tubes with the same geometric characteristics, Exp. Therm. Fluid Sci. 35 (2011) 832–840.
[83] L.M. Schlager, M.B. Pate, A.E. Bergles, Evaporation and condensation heat transfer and pressure drop in horizontal, 12.7-mm microfin tubes with refrigerant 22, J. Heat Transfer 112 (1990) 1041–1047.

[84] M.-H. Kim, J.-S. Shin, Evaporating heat transfer of R22 and R410A in horizontal smooth and microfin tubes, Int. J. Refrig. 28 (2005) 940–948.
[85] L.M. Chamra, R.L. Webb, M.R. Randlett, Advanced micro-fin tubes for evaporation, Int. J. Heat Mass Transfer 39 (1996) 1827–1838.
[86] K. Spindler, H. Müller-Steinhagen, Flow boiling heat transfer of R134a and R404A in a microfin tube at low mass fluxes and low heat fluxes, Heat Mass Transfer 45 (2009) 967–977.
[87] M.-H. Yu, T.-K. Lin, C.-C. Tseng, Heat transfer and flow pattern during two-phase flow boiling of R-134a in horizontal smooth and microfin tubes, Int. J. Refrig. 25 (2002) 789–798.
[88] W. Cui, L. Li, M. Xin, T.-C. Jen, Q. Liao, Q. Chen, An experimental study of flow pattern and pressure drop for flow boiling inside microfinned helically coiled tube, Int. J. Heat Mass Transfer 51 (2008) 169–175.
[89] W. Cui, L. Li, M. Xin, T.-C. Jen, Q. Chen, Q. Liao, A heat transfer correlation of flow boiling in micro-finned helically coiled tube, Int. J. Heat Mass Transfer 49 (2006) 2851–2858.
[90] B. Soleimani, A. Keshavarz, Heat transfer enhancement of an internal subcooled flow boiling over a hot spot, Appl. Therm. Eng. 99 (2016) 206–213.
[91] L. Cheng, T. Chen, Study of flow boiling heat transfer in a tube with axial microgrooves, Exp. Heat Transfer 14 (2001) 59–73.
[92] W.-L. Cheng, H. Chen, S. Yuan, Q. Zhong, Y.-F. Fan, Experimental study on heat transfer characteristics of R134a flow boiling in "Ω"-shaped grooved tube with different flow directions, Int. J. Heat Mass Transfer 108 (2017) 988–997.
[93] M.A. Abdous, H. Saffari, H. Barzegar Avval, M. Khoshzat, The study of entropy generation during flow boiling in a micro-fin tube, Int. J. Refrig. 68 (2016) 76–93.
[94] S. Mancin, A. Diani, L. Rossetto, Experimental measurements of R134a flow boiling inside a 3.4-mm ID microfin tube, Heat Transfer Eng. 36 (2015) 1218–1229.
[95] S. Mancin, A. Diani, L. Rossetto, R134a flow boiling heat transfer and pressure drop inside a 3.4mm ID microfin tube, Energy Procedia 45 (2014) 608–615.
[96] Z. Wu, Y. Wu, B. Sundén, W. Li, Convective vaporization in micro-fin tubes of different geometries, Exp. Therm. Fluid Sci. 44 (2013) 398–408.
[97] L. Gao, T. Honda, S. Koyama, Experiments on flow boiling heat transfer of almost pure CO_2 and CO_2-oil mixtures in horizontal smooth and microfin tubes, HVAC&R Res. 13 (2007) 415–425.
[98] A. Padovan, D.D. Col, L. Rossetto, Experimental study on flow boiling of R134a and R410A in a horizontal microfin tube at high saturation temperatures, Appl. Therm. Eng. 31 (2011) 3814–3826.
[99] A.-E. Schael, M. Kind, Flow pattern and heat transfer characteristics during flow boiling of CO_2 in a horizontal micro fin tube and comparison with smooth tube data, Int. J. Refrig. 28 (2005) 1186–1195.
[100] C. Dang, N. Haraguchi, E. Hihara, Flow boiling heat transfer of carbon dioxide inside a small-sized microfin tube, Int. J. Refrig. 33 (2010) 655–663.
[101] J. Wongsa-ngam, T. Nualboonrueng, S. Wongwises, Performance of smooth and micro-fin tubes in high mass flux region of R-134a during evaporation, Heat Mass Transfer 40 (2004) 425–435.
[102] A. Singh, M.M. Ohadi, S. Dessiatoun, Flow boiling heat transfer coefficients of R-134a in a microfin tube, J. Heat Transfer 118 (1996) 497–499.
[103] J.C. Passos, V.F. Kuser, P. Haberschill, M. Lallemand, Convective boiling of R-407c inside horizontal microfin and plain tubes, Exp. Therm. Fluid Sci. 27 (2003) 705–713.
[104] X. Han, P. Li, Z. Wang, X. Wang, X. Zhang, G. Chen, Evaporation heat transfer and pressure drop of R161 in a 7mm micro-fin tube, Int. J. Heat Mass Transfer 62 (2013) 638–646.
[105] K. Seo, Y. Kim, Evaporation heat transfer and pressure drop of R-22 in 7 and 9.52 mm smooth/micro-fin tubes, Int. J. Heat Mass Transfer 43 (2000) 2869–2882.
[106] Y. Kim, K. Seo, J.T. Chung, Evaporation heat transfer characteristics of R-410A in 7 and 9.52 mm smooth/micro-fin tubes, Int. J. Refrig. 25 (2002) 716–730.
[107] J.M. Cho, M.S. Kim, Experimental studies on the evaporative heat transfer and pressure drop of CO_2 in smooth and micro-fin tubes of the diameters of 5 and 9.52mm, Int. J. Refrig. 30 (2007) 986–994.
[108] Y.J. Kim, J.M. Cho, M.S. Kim, Experimental study on the evaporative heat transfer and pressure drop of CO_2 flowing upward in vertical smooth and micro-fin tubes with the diameter of 5mm, Int. J. Refrig. 31 (2008) 771–779.
[109] J.M. Cho, Y.J. Kim, M.S. Kim, Experimental studies on the evaporative heat transfer and pressure drop of CO_2 and CO_2/propane mixtures flowing upward in smooth and micro-fin tubes with outer diameter of 5mm for an inclination angle of 45°, Int. J. Refrig. 33 (2010) 922–931.
[110] C.S. Kuo, C.C. Wang, In-tube evaporation of HCFC-22 in a 9.52 mm micro-fin/smooth tube, Int. J. Heat Mass Transfer 39 (1996) 2559–2569.
[111] S.-S. Hsieh, M.-Y. Wen, An experimental study of flow boiling heat transfer in rib-roughened tube annuli, J. Heat Transfer 117 (1995) 185–194.
[112] H. Hu, G. Ding, K. Wang, Heat transfer characteristics of R410A–oil mixture flow boiling inside a 7mm straight microfin tube, Int. J. Refrig. 31 (2008) 1081–1093.
[113] O. Zürcher, J.R. Thome, D. Favrat, In-tube flow boiling of R-407C and R-407C/oil mixtures Part I: microfin tube, HVAC&R Res. 4 (1998) 347–372.
[114] W. Targanski, J.T. Cieslinski, Evaporation of R407C/oil mixtures inside corrugated and micro-fin tubes, Appl. Therm. Eng. 27 (2007) 2226–2232.
[115] X. Han, P. Li, X. Yuan, Q. Wang, G. Chen, The boiling heat transfer characteristics of the mixture HFO-1234yf/oil inside a micro-fin tube, Int. J. Heat Mass Transfer 67 (2013) 1122–1130.
[116] E. Nidegger, J.R. Thome, D. Favrat, Flow boiling and pressure drop measurements for R-134a/oil mixtures Part 1: evaporation in a microfin tube, HVAC&R Res. 3 (1997) 38–53.
[117] H.-T. Hu, G.-L. Ding, K.-J. Wang, Measurement and correlation of frictional two-phase pressure drop of R410A/POE oil mixture flow boiling in a 7mm straight micro-fin tube, Appl. Therm. Eng. 28 (2008) 1272–1283.
[118] C. Kondou, D. BaBa, F. Mishima, S. Koyama, Flow boiling of non-azeotropic mixture R32/R1234ze(E) in horizontal microfin tubes, Int. J. Refrig. 36 (2013) 2366–2378.
[119] C.-S. Kuo, C.-C. Wang, Horizontal flow boiling of R22 and R407C in a 9.52 mm micro-fin tube, Appl. Therm. Eng. 16 (1996) 719–731.
[120] A. Diani, S. Mancin, A. Cavallini, L. Rossetto, Experimental investigation of R1234ze(E) flow boiling inside a 2.4 mm ID horizontal microfin tube, Int. J. Refrig. 69 (2016) 272–284.
[121] A. Diani, S. Mancin, L. Rossetto, R1234ze(E) flow boiling inside a 3.4 mm ID microfin tube, Int. J. Refrig. 47 (2014) 105–119.
[122] A. Diani, S. Mancin, L. Rossetto, Flow boiling heat transfer of R1234yf inside a 3.4mm ID microfin tube, Exp. Therm. Fluid Sci. 66 (2015) 127–136.
[123] A.D. Sommers, K.L. Yerkes, Using micro-structural surface features to enhance the convective flow boiling heat transfer of R-134a on aluminum, Int. J. Heat Mass Transfer 64 (2013) 1053–1063.
[124] W. Lee, G. Son, H.Y. Yoon, Direct numerical simulation of flow boiling in a finned microchannel, Int. Commun. Heat Mass Transfer 39 (2012) 1460–1466.
[125] R. Yun, Y. Kim, K. Seo, H.Y. Kim, A generalized correlation for evaporation heat transfer of refrigerants in micro-fin tubes, Int. J. Heat Mass Transfer 45 (2002) 2003–2010.
[126] H. Honda, Y.S. Wang, Theoretical study of evaporation heat transfer in horizontal microfin tubes: stratified flow model, Int. J. Heat Mass Transfer 47 (2004) 3971–3983.
[127] O. Makishi, H. Honda, Y.S. Wang, New theoretical models of evaporation heat transfer in horizontal microfin tubes, Int. J. Heat Mass Transfer 49 (2006) 2328–2336.
[128] X. Zhang, X. Yuan, Heat transfer correlations for evaporation of refrigerant mixtures flowing inside horizontal microfin tubes, Energy Convers. Manage. 49 (2008) 3198–3204.
[129] R. Merchant, S. Mehendale, A new model for predicting flow boiling heat transfer coefficients in horizontal microfin tubes, in: Proceedings of the ASME 2016 International Mechanical Engineering Congress and Exposition, ASME, Phoenix, USA, 2016.
[130] Y. Haramura, Y. Katto, A new hydrodynamic model of critical heat flux, applicable widely to both pool and forced convection boiling on submerged bodies in saturated liquids, Int. J. Heat Mass Transfer 26 (1983) 389–399.
[131] D.A. McNeil, A.H. Raeisi, P.A. Kew, P.R. Bobbili, A comparison of flow boiling heat-transfer in in-line mini pin fin and plane channel flows, Appl. Therm. Eng. 30 (2010) 2412–2425.
[132] Y.J. Lee, P.S. Lee, S.K. Chou, Numerical study of fluid flow and heat transfer in the enhanced microchannel with oblique fins, J. Heat Transfer 135 (2013) 041901.
[133] Y.J. Lee, P.S. Lee, S.K. Chou, Enhanced thermal transport in microchannel using oblique fins, J. Heat Transfer 134 (2012) 101901.
[134] M. Law, P.-S. Lee, K. Balasubramanian, Experimental investigation of flow boiling heat transfer in novel oblique-finned microchannels, Int. J. Heat Mass Transfer 76 (2014) 419–431.
[135] M. Law, P.-S. Lee, A comparative study of experimental flow boiling heat transfer and pressure characteristics in straight- and oblique-finned microchannels, Int. J. Heat Mass Transfer 85 (2015) 797–810.
[136] T.J. Cognata, D.K. Hollingsworth, L.C. Witte, High-speed visualization of two-phase flow in a micro-scale pin-fin heat exchanger, Heat Transfer Eng. 28 (2007) 861–869.
[137] A. Reeser, A. Bar-Cohen, G. Hetsroni, High quality flow boiling heat transfer and pressure drop in microgap pin fin arrays, Int. J. Heat Mass Transfer 78 (2014) 974–985.
[138] W. Qu, A. Siu-Ho, Experimental study of saturated flow boiling heat transfer in an array of staggered micro-pin-fins, Int. J. Heat Mass Transfer 52 (2009) 1853–1863.
[139] W. Qu, A. Siu-Ho, Measurement and prediction of pressure drop in a two-phase micro-pin-fin heat sink, Int. J. Heat Mass Transfer 52 (2009) 5173–5184.
[140] C. Woodcock, X. Yu, J. Plawsky, Y. Peles, Piranha Pin Fin (PPF) — Advanced flow boiling microstructures with low surface tension dielectric fluids, Int. J. Heat Mass Transfer 90 (2015) 591–604.
[141] X. Yu, C. Woodcock, Y. Wang, J. Plawsky, Y. Peles, A comparative study of flow boiling in a microchannel with piranha pin fins, J. Heat Transfer 138 (2016) 111502.
[142] X. Yu, C. Woodcock, Y. Wang, J. Plawsky, Y. Peles, Enhanced subcooled flow boiling heat transfer in microchannel with piranha pin fin, J. Heat Transfer 139 (2017) 112402.
[143] S. Krishnamurthy, Y. Peles, Flow boiling of water in a circular staggered micro-pin fin heat sink, Int. J. Heat Mass Transfer 51 (2008) 1349–1364.
[144] S. Krishnamurthy, Y. Peles, Flow boiling heat transfer on micro pin fins entrenched in a microchannel, J. Heat Transfer 132 (2010) 041007.
[145] S. Krishnamurthy, Y. Peles, Flow boiling on micropin fins entrenched inside a microchannel—flow patterns and bubble departure diameter and bubble frequency, J. Heat Transfer 132 (2010) 041002.

[146] A. Koşar, Y. Peles, Boiling heat transfer in a hydrofoil-based micro pin fin heat sink, Int. J. Heat Mass Transfer 50 (2007) 1018–1034.
[147] A. Ma, J. Wei, M. Yuan, J. Fang, Enhanced flow boiling heat transfer of FC-72 on micro-pin-finned surfaces, Int. J. Heat Mass Transfer 52 (2009) 2925–2931.
[148] M. Yuan, J. Wei, Y. Xue, J. Fang, Subcooled flow boiling heat transfer of FC-72 from silicon chips fabricated with micro-pin-fins, Int. J. Therm. Sci. 48 (2009) 1416–1422.
[149] Y.M. Lie, J.H. Ke, W.R. Chang, T.C. Cheng, T.F. Lin, Saturated flow boiling heat transfer and associated bubble characteristics of FC-72 on a heated micro-pin-finned silicon chip, Int. J. Heat Mass Transfer 50 (2007) 3862–3876.
[150] W.R. Chang, C.A. Chen, J.H. Ke, T.F. Lin, Subcooled flow boiling heat transfer and associated bubble characteristics of FC-72 on a heated micro-pin-finned silicon chip, Int. J. Heat Mass Transfer 53 (2010) 5605–5621.
[151] D. Deng, W. Wan, Y. Qin, J. Zhang, X. Chu, Flow boiling enhancement of structured microchannels with micro pin fins, Int. J. Heat Mass Transfer 105 (2017) 338–349.
[152] W. Wan, D. Deng, Q. Huang, T. Zeng, Y. Huang, Experimental study and optimization of pin fin shapes in flow boiling of micro pin fin heat sinks, Appl. Therm. Eng. 114 (2017) 436–449.
[153] Y. Zhu, D.S. Antao, K.-H. Chu, S. Chen, T.J. Hendricks, T. Zhang, E.N. Wang, Surface structure enhanced microchannel flow boiling, J. Heat Transfer 138 (2016) 091501.
[154] Y. Zhu, D.S. Antao, D.W. Bian, S.R. Rao, J.D. Sircar, T. Zhang, E.N. Wang, Suppressing high-frequency temperature oscillations in microchannels with surface structures, Appl. Phys. Lett. 110 (2017) 033501.
[155] S. Bigham, A. Fazeli, S. Moghaddam, Physics of microstructures enhancement of thin film evaporation heat transfer in microchannels flow boiling, Sci. Rep. 7 (2017) 44745.
[156] C.-D. Wen, I. Mudawar, Emissivity characteristics of polished aluminum alloy surfaces and assessment of multispectral radiation thermometry (MRT) emissivity models, Int. J. Heat Mass Transfer 48 (2005) 1316.
[157] C.J. Kuo, Y. Peles, Flow boiling of coolant (HFE-7000) inside structured and plain wall microchannels, J. Heat Transfer 131 (2009) 121011.
[158] C.J. Kuo, Y. Peles, Local measurement of flow boiling in structured surface microchannels, Int. J. Heat Mass Transfer 50 (2007) 4513–4526.
[159] A. Koşar, C.-J. Kuo, Y. Peles, Boiling heat transfer in rectangular microchannels with reentrant cavities, Int. J. Heat Mass Transfer 48 (2005) 4867–4886.
[160] A. Koşar, C.-J. Kuo, Y. Peles, Reduced pressure boiling heat transfer in rectangular microchannels with interconnected reentrant cavities, J. Heat Transfer 127 (2005) 1106–1114.
[161] P.H. Lin, B.R. Fu, C. Pan, Critical heat flux on flow boiling of methanol–water mixtures in a diverging microchannel with artificial cavities, Int. J. Heat Mass Transfer 54 (2011) 3156–3166.
[162] M. Piasecka, An application of enhanced heating surface with mini-reentrant cavities for flow boiling research in minichannels, Heat Mass Transfer 49 (2013) 261–275.
[163] M. Piasecka, Heat transfer mechanism, pressure drop and flow patterns during FC-72 flow boiling in horizontal and vertical minichannels with enhanced walls, Int. J. Heat Mass Transfer 66 (2013) 472–488.
[164] M. Piasecka, The use of enhanced surface in flow boiling heat transfer in a rectangular minichannel, Exp. Heat Transfer 27 (2014) 231–255.
[165] Y. Li, G. Xia, Y. Jia, Y. Cheng, J. Wang, Experimental investigation of flow boiling performance in microchannels with and without triangular cavities – A comparative study, Int. J. Heat Mass Transfer 108 (2017) 1511–1526.
[166] R. Rioboo, M. Marengo, S. Dall'Olio, M. Voue, J. De, Coninck, An innovative method to control the incipient flow boiling through grafted surfaces with chemical patterns, Langmuir 25 (2009) 6005–6009.
[167] J. Zeng, S. Zhang, Y. Tang, Y. Sun, W. Yuan, Flow boiling characteristics of micro-grooved channels with reentrant cavity array at different operational conditions, Int. J. Heat Mass Transfer 114 (2017) 1001–1012.
[168] A. Sitar, I. Golobic, Effect of nucleation cavities on enhanced boiling heat transfer in microchannels, Nanoscale Microscale Thermophys. Eng. 20 (2016) 33–50.
[169] S.-S. Hsieh, C.-Y. Lin, Subcooled convective boiling in structured surface microchannels, J. Micromech. Microeng. 20 (2010) 015027.
[170] C.N. Ammerman, S.M. You, Enhancing small-channel convective boiling performance using a microporous surface coating, J. Heat Transfer 123 (2001) 976–983.
[171] K.N. Rainey, G. Li, S.M. You, Flow boiling heat transfer from plain and microporous coated surfaces in subcooled FC-72, J. Heat Transfer 123 (2001) 918–925.
[172] M.S. Sarwar, Y.H. Jeong, S.H. Chang, Subcooled flow boiling CHF enhancement with porous surface coatings, Int. J. Heat Mass Transfer 50 (2007) 3649–3657.
[173] I. Pranoto, K.C. Leong, An experimental study of flow boiling heat transfer from porous foam structures in a channel, Appl. Therm. Eng. 70 (2014) 100–114.
[174] C.Y. Zhao, W. Lu, S.A. Tassou, Flow boiling heat transfer in horizontal metal-foam tubes, J. Heat Transfer 131 (2009) 121002.
[175] Z.Q. Chen, P. Cheng, T.S. Zhao, An experimental study of two phase flow and boiling heat transfer in bi-dispersed porous channels, Int. Commun. Heat Mass Transfer 27 (2000) 293–302.
[176] D. Deng, W. Wan, Y. Tang, Z. Wan, D. Liang, Experimental investigations on flow boiling performance of reentrant and rectangular microchannels – A comparative study, Int. J. Heat Mass Transfer 82 (2015) 435–446.
[177] D. Deng, Y. Tang, D. Liang, H. He, S. Yang, Flow boiling characteristics in porous heat sink with reentrant microchannels, Int. J. Heat Mass Transfer 70 (2014) 463–477.
[178] D. Deng, Y. Tang, H. Shao, J. Zeng, W. Zhou, D. Liang, Effects of structural parameters on flow boiling performance of reentrant porous microchannels, J. Micromech. Microeng. 24 (2014) 065025.
[179] D. Deng, R. Chen, H. He, J. Feng, Y. Tang, W. Zhou, Effects of heat flux, mass flux and channel size on flow boiling performance of reentrant porous microchannels, Exp. Therm. Fluid Sci. 64 (2015) 13–22.
[180] D. Deng, R. Chen, Y. Tang, L. Lu, T. Zeng, W. Wan, A comparative study of flow boiling performance in reentrant copper microchannels and reentrant porous microchannels with multi-scale rough surface, Int. J. Multiphase Flow 72 (2015) 275–287.
[181] D. Deng, W. Wan, H. Shao, Y. Tang, J. Feng, J. Zeng, Effects of operation parameters on flow boiling characteristics of heat sink cooling systems with reentrant porous microchannels, Energy Convers. Manage. 96 (2015) 340–351.
[182] D. Deng, Y. Xie, Q. Huang, W. Wan, On the flow boiling enhancement in interconnected reentrant microchannels, Int. J. Heat Mass Transfer 108 (2017) 453–467.
[183] P. Bai, T. Tang, B. Tang, Enhanced flow boiling in parallel microchannels with metallic porous coating, Appl. Therm. Eng. 58 (2013) 291–297.
[184] Y. Sun, L. Zhang, H. Xu, X. Zhong, Flow boiling enhancement of FC-72 from microporous surfaces in minichannels, Exp. Therm. Fluid Sci. 35 (2011) 1418–1426.
[185] Y. Sun, L. Zhang, H. Xu, X. Zhong, Subcooled flow boiling heat transfer from microporous surfaces in a small channel, Int. J. Therm. Sci. 50 (2011) 881–889.
[186] S. Zhang, W. Yuan, Y. Tang, J. Chen, Z. Li, Enhanced flow boiling in an interconnected microchannel net at different inlet subcooling, Appl. Therm. Eng. 104 (2016) 659–667.
[187] Y. Tang, C. Chen, S. Zhang, Y. Sun, J. Zeng, W. Yuan, Z. Li, Effects of structural parameter on flow boiling performance of interconnected microchannel net, Appl. Therm. Eng. 112 (2017) 164–173.
[188] S. Zhang, Y. Tang, W. Yuan, J. Zeng, Y. Xie, A comparative study of flow boiling performance in the interconnected microchannel net and rectangular microchannels, Int. J. Heat Mass Transfer 98 (2016) 814–823.
[189] S. Zhang, Y. Sun, W. Yuan, Y. Tang, H. Tang, K. Tang, Effects of heat flux, mass flux and channel width on flow boiling performance of porous interconnected microchannel nets, Exp. Therm. Fluid Sci. 90 (2018) 310–318.
[190] A. Megahed, Experimental investigation of flow boiling characteristics in a cross-linked microchannel heat sink, Int. J. Multiphase Flow 37 (2011) 380–393.
[191] H. Wang, R.B. Peterson, Enhanced boiling heat transfer in parallel microchannels with diffusion brazed wire mesh, IEEE Trans. Compon. Packag. Technol. 33 (2010) 784–793.
[192] B. Dawidowicz, J.T. Cieśliński, Heat transfer and pressure drop during flow boiling of pure refrigerants and refrigerant/oil mixtures in tube with porous coating, Int. J. Heat Mass Transfer 55 (2012) 2549–2558.
[193] W. Cui, S.K. Mungai, C. Wilson, H. Ma, B. Li, Subcooled flow boiling on a two-step electrodeposited copper porous surface, J. Enhanced Heat Transfer 23 (2016) 91–107.
[194] J.W. Palko, H. Lee, C. Zhang, T.J. Dusseault, T. Maitra, Y. Won, D.D. Agonafer, J. Moss, F. Houshmand, G. Rong, J.D. Wilbur, D. Rockosi, I. Mykyta, D. Resler, D. Altman, M. Asheghi, J.G. Santiago, K.E. Goodson, Extreme two-phase cooling from laser-etched diamond and conformal, template-fabricated microporous copper, Adv. Funct. Mater. 27 (2017) 1703265.
[195] B.-R. Fu, S.-Y. Chung, W.-J. Lin, L. Wang, C. Pan, Critical heat flux enhancement of HFE-7100 flow boiling in a minichannel heat sink with saw-tooth structures, Adv. Mech. Eng. 9 (2017) 1–10.
[196] S.-Y. Chung, C. Pan, The enhancement of boiling heat transfer in a minichannel heat sink with saw-tooth structure on channel surface, in: Proceedings of the ASME 2016 5th International Conference on Micro/Nanoscale Heat and Mass Transfer, Biopolis, Singapore, 2016.
[197] H.Z. Cao, H.B. Xu, N. Liang, C.Q. Tian, Experiment investigation of R134a flow boiling process in microchannel with cavitation structure, Heat Transfer Eng. 32 (2011) 542–553.
[198] H.S. Ahn, S.H. Kang, C. Lee, J. Kim, M.H. Kim, The effect of liquid spreading due to micro-structures of flow boiling critical heat flux, Int. J. Multiphase Flow 43 (2012) 1–12.
[199] V. Khanikar, I. Mudawar, T. Fisher, Effects of carbon nanotube coating on flow boiling in a micro-channel, Int. J. Heat Mass Transfer 52 (2009) 3805–3817.
[200] V. Khanikar, I. Mudawar, T.S. Fisher, Flow boiling in a micro-channel coated with carbon nanotubes, IEEE Trans. Compon. Packag. Technol. 32 (2009) 639–649.
[201] C.S.S. Kumar, S. Suresh, L. Yang, Q. Yang, S. Aravind, Flow boiling heat transfer enhancement using carbon nanotube coatings, Appl. Therm. Eng. 65 (2014) 166–175.
[202] N. Singh, V. Sathyamurthy, W. Peterson, J. Arendt, D. Banerjee, Flow boiling enhancement on a horizontal heater using carbon nanotube coatings, Int. J. Heat Fluid Flow 31 (2010) 201–207.
[203] A.S. Kousalya, C.N. Hunter, S.A. Putnam, T. Miller, T.S. Fisher, Photonically enhanced flow boiling in a channel coated with carbon nanotubes, Appl. Phys. Lett. 100 (2012) 071601.

[204] A.K.M.M. Morshed, F. Yang, M. Yakut Ali, J.A. Khan, C. Li, Enhanced flow boiling in a microchannel with integration of nanowires, Appl. Therm. Eng. 32 (2012) 68–75.
[205] D. Li, G.S. Wu, W. Wang, Y.D. Wang, D. Liu, D.C. Zhang, Y.F. Chen, G.P. Peterson, R. Yang, Enhancing flow boiling heat transfer in microchannels for thermal management with monolithically-integrated silicon nanowires, Nano Lett. 12 (2012) 3385–3390.
[206] F. Yang, W. Li, X. Dai, C. Li, Flow boiling heat transfer of HFE-7000 in nanowire-coated microchannels, Appl. Therm. Eng. 93 (2016) 260–268.
[207] F. Yang, X. Dai, Y. Peles, P. Cheng, J. Khan, C. Li, Flow boiling phenomena in a single annular flow regime in microchannels (I): Characterization of flow boiling heat transfer, Int. J. Heat Mass Transfer 68 (2014) 703–715.
[208] F. Yang, X. Dai, Y. Peles, P. Cheng, J. Khan, C. Li, Flow boiling phenomena in a single annular flow regime in microchannels (II): Reduced pressure drop and enhanced critical heat flux, Int. J. Heat Mass Transfer 68 (2014) 716–724.
[209] T. Alam, W. Li, F. Yang, W. Chang, J. Li, Z. Wang, J. Khan, C. Li, Force analysis and bubble dynamics during flow boiling in silicon nanowire microchannels, Int. J. Heat Mass Transfer 101 (2016) 915–926.
[210] T. Alam, A.S. Khan, W. Li, F. Yang, Y. Tong, J. Khan, C. Li, Transient force analysis and bubble dynamics during flow boiling in silicon nanowire microchannels, Int. J. Heat Mass Transfer 101 (2016) 937–947.
[211] T. Alam, W. Li, F. Yang, J. Khan, C. Li, Orientation effects on flow boiling silicon nanowire microchannels, in: Proceedings of the ASME 2016 5th International Conference on Micro/Nanoscale Heat and Mass Transfer, Biopolis, Singapore, 2016.
[212] S. Shin, G. Choi, B.S. Kim, H.H. Cho, Flow boiling heat transfer on nanowire-coated surfaces with highly wetting liquid, Energy 76 (2014) 428–435.
[213] D.P. Ghosh, D. Sharma, D. Mohanty, S.K. Saha, R. Raj, Facile fabrication of nanostructured microchannels for flow boiling heat transfer enhancement, Heat Transfer Eng. (2018) 1–12.
[214] E. Demir, T. İzci, W.J. Khudhayer, A.S. Alagöz, T. Karabacak, A. Koşar, The effect of nanostructure distribution on subcooled boiling heat transfer enhancement over nanostructured plates integrated into a rectangular channel, Nanoscale Microscale Thermophys. Eng. 18 (2014) 313–328.
[215] Y.J. Choi, D.H. Kam, Y.H. Jeong, Analysis of CHF enhancement by magnetite nanoparticle deposition in the subcooled flow boiling region, Int. J. Heat Mass Transfer 109 (2017) 1191–1199.
[216] H.S. Ahn, S.H. Kang, H. Jo, H. Kim, M.H. Kim, Visualization study of the effects of nanoparticles surface deposition on convective flow boiling CHF from a short heated wall, Int. J. Multiphase Flow 37 (2011) 215–228.
[217] A.K.M.M. Morshed, T.C. Paul, J.A. Khan, Effect of Al_2O_3 nanoparticle deposition on flow boiling performance of water in a microchannel, Exp. Therm. Fluid Sci. 47 (2013) 6–13.
[218] H.S. Ahn, S.H. Kang, M.H. Kim, Visualized effect of alumina nanoparticles surface deposition on water flow boiling heat transfer, Exp. Therm. Fluid Sci. 37 (2012) 154–163.
[219] A.K.M.M. Morshed, T.C. Paul, J. Khan, Effect of Cu–Al_2O_3 nanocomposite coating on flow boiling performance of a microchannel, Appl. Therm. Eng. 51 (2013) 1135–1143.
[220] A.K.M.M. Morshed, T.C. Paul, J.A. Khan, Effect of cross groove on flow boiling in a microgap, in: Proceedings of the ASME 2012 Summer Heat Transfer Conference, ASME, Rio Grande, Puerto Rico, 2012, pp. 457–463.
[221] M.-Y. Liu, H. Wang, Y. Wang, Enhancing flow boiling and antifouling with nanometer titanium dioxide coating surfaces, AIChE J. 53 (2007) 1075–1085.
[222] C.S.S. Kumar, S. Suresh, Q. Yang, C.R. Aneesh, An experimental investigation on flow boiling heat transfer enhancement using spray pyrolysed alumina porous coatings, Appl. Therm. Eng. 71 (2014) 508–518.
[223] C.S.S. Kumar, S. Suresh, C.R. Aneesh, M.C.S. Kumar, A.S. Praveen, K. Raji, Flow boiling heat transfer enhancement on copper surface using Fe doped Al_2O_3–TiO_2 composite coatings, Appl. Surf. Sci. 334 (2015) 102–109.
[224] C.S.S. Kumar, S. Suresh, A.S. Praveen, M.C. Santhosh Kumar, V. Gopi, Effect of surfactant addition on hydrophilicity of ZnO–Al_2O_3 composite and enhancement of flow boiling heat transfer, Exp. Therm. Fluid Sci. 70 (2016) 325–334.
[225] T. Çıkım, E. Armağan, G. Ozaydin Ince, A. Koşar, Flow boiling enhancement in microtubes with crosslinked pHEMA coatings and the effect of coating thickness, J. Heat Transfer 136 (2014) 081504.
[226] M. Nedaei, A.R. Motezakker, M.C. Zeybek, M. Sezen, G.O. Ince, A. Kosar, Subcooled flow boiling heat transfer enhancement using polyperfluorodecylacrylate (pPFDA) coated microtubes with different coating thicknesses, Exp. Therm. Fluid Sci. 86 (2017) 130–140.
[227] C. Choi, J.S. Shin, D.I. Yu, M.H. Kim, Flow boiling behaviors in hydrophilic and hydrophobic microchannels, Exp. Therm. Fluid Sci. 35 (2011) 816–824.
[228] H.T. Phan, N. Caney, P. Marty, S. Colasson, J. Gavillet, Flow boiling of water in a minichannel: the effects of surface wettability on two-phase pressure drop, Appl. Therm. Eng. 31 (2011) 1894–1905.
[229] K. Zhou, C. Coyle, J. Li, J. Buongiorno, W. Li, Flow boiling in vertical narrow microchannels of different surface wettability characteristics, Int. J. Heat Mass Transfer 109 (2017) 103–114.
[230] W. Li, K. Zhou, J. Li, Z. Feng, H. Zhu, Effects of heat flux, mass flux and two-phase inlet quality on flow boiling in a vertical superhydrophilic microchannel, Int. J. Heat Mass Transfer 119 (2018) 601–613.
[231] R. Ahmadi, T. Okawa, Influence of surface wettability on bubble behavior and void evolution in subcooled flow boiling, Int. J. Therm. Sci. 97 (2015) 114–125.
[232] A.S. Kousalya, K.P. Singh, T.S. Fisher, Heterogeneous wetting surfaces with graphitic petal-decorated carbon nanotubes for enhanced flow boiling, Int. J. Heat Mass Transfer 87 (2015) 380–389.
[233] J.M. Kim, T. Kim, D.I. Yu, H. Noh, M.H. Kim, K. Moriyama, H.S. Park, Effect of heterogeneous wetting surface characteristics on flow boiling performance, Int. J. Heat Fluid Flow 70 (2018) 141–151.
[234] I. Mudawar, T.M. Anderson, Optimization of enhanced surfaces for high flux chip cooling by pool boiling, J. Electron. Packag. 115 (1993) 89–100.
[235] W. Qu, I. Mudawar, Measurement and prediction of pressure drop in two-phase micro-channel heat sinks, Int. J. Heat Mass Transfer 46 (2003) 2737–2753.
[236] H.Y. Wu, P. Cheng, Boiling instability in parallel silicon microchannels at different heat flux, Int. J. Heat Mass Transfer 47 (2004) 3631–3641.
[237] G. Wang, P. Cheng, H. Wu, Unstable and stable flow boiling in parallel microchannels and in a single microchannel, Int. J. Heat Mass Transfer 50 (2007) 4297–4310.
[238] C. Huh, J. Kim, M.H. Kim, Flow pattern transition instability during flow boiling in a single microchannel, Int. J. Heat Mass Transfer 50 (2007) 1049–1060.
[239] G. Wang, P. Cheng, A.E. Bergles, Effects of inlet/outlet configurations on flow boiling instability in parallel microchannels, Int. J. Heat Mass Transfer 51 (2008) 2267–2281.
[240] H.J. Lee, D.Y. Liu, S.-C. Yao, Flow instability of evaporative micro-channels, Int. J. Heat Mass Transfer 53 (2010) 1740–1749.
[241] B.A. Odom, M.J. Miner, C.A. Ortiz, J.A. Sherbeck, R.S. Prasher, P.E. Phelan, Microchannel two-phase flow oscillation control with an adjustable inlet orifice, J. Heat Transfer 134 (2012) 122901.
[242] A. Sitar, I. Sedmak, I. Golobic, Boiling of water and FC-72 in microchannels enhanced with novel features, Int. J. Heat Mass Transfer 55 (2012) 6446–6457.
[243] A. Koşar, C.-J. Kuo, Y. Peles, Suppression of boiling flow oscillations in parallel microchannels by inlet restrictors, J. Heat Transfer 128 (2005) 251–260.
[244] T. Zhang, Y. Peles, J.T. Wen, T. Tong, J.-Y. Chang, R. Prasher, M.K. Jensen, Analysis and active control of pressure-drop flow instabilities in boiling microchannel systems, Int. J. Heat Mass Transfer 53 (2010) 2347–2360.
[245] C.T. Lu, C. Pan, Stabilization of flow boiling in microchannel heat sinks with a diverging cross-section design, J. Micromech. Microeng. 18 (2008) 075035.
[246] P.C. Lee, C. Pan, Boiling heat transfer and two-phase flow of water in a single shallow microchannel with a uniform or diverging cross section, J. Micromech. Microeng. 18 (2008) 025005.
[247] C.T. Lu, C. Pan, A highly stable microchannel heat sink for convective boiling, J. Micromech. Microeng. 19 (2009) 055013.
[248] C.T. Lu, C. Pan, Convective boiling in a parallel microchannel heat sink with a diverging cross section and artificial nucleation sites, Exp. Therm. Fluid Sci. 35 (2011) 810–815.
[249] B.R. Fu, M.S. Tsou, C. Pan, Boiling heat transfer and critical heat flux of ethanol–water mixtures flowing through a diverging microchannel with artificial cavities, Int. J. Heat Mass Transfer 55 (2012) 1807–1814.
[250] K. Balasubramanian, P.S. Lee, L.W. Jin, S.K. Chou, C.J. Teo, S. Gao, Experimental investigations of flow boiling heat transfer and pressure drop in straight and expanding microchannels – A comparative study, Int. J. Therm. Sci. 50 (2011) 2413–2421.
[251] S. Hardt, S. Herbert, C. Kunkelmann, S. Mahjoob, P. Stephan, Unidirectional bubble growth in microchannels with asymmetric surface features, Int. J. Heat Mass Transfer 55 (2012) 7056–7062.
[252] S. Hong, Y. Tang, Y. Lai, S. Wang, An experimental investigation on effect of channel configuration in ultra-shallow micro multi-channels flow boiling: Heat transfer enhancement and visualized presentation, Exp. Therm. Fluid Sci. 83 (2017) 239–247.
[253] Y.K. Prajapati, M. Pathak, M. Kaleem Khan, A comparative study of flow boiling heat transfer in three different configurations of microchannels, Int. J. Heat Mass Transfer 85 (2015) 711–722.
[254] M.J. Miner, P.E. Phelan, B.A. Odom, C.A. Ortiz, R.S. Prasher, J.A. Sherbeck, Optimized expanding microchannel geometry for flow boiling, J. Heat Transfer 135 (2013) 042901.
[255] M.J. Miner, P.E. Phelan, B.A. Odom, C.A. Ortiz, An experimental investigation of pressure drop in expanding microchannel arrays, J. Heat Transfer 136 (2013) 031502.
[256] M.J. Miner, P.E. Phelan, B.A. Odom, C.A. Ortiz, Experimental measurements of critical heat flux in expanding microchannel arrays, J. Heat Transfer 135 (2013) 101501.
[257] M.J. Miner, P.E. Phelan, Effect of cross-sectional perturbation on critical heat flux criteria in microchannels, J. Heat Transfer 135 (2013) 101009.
[258] M.K. Sung, I. Mudawar, Single-phase and two-phase heat transfer characteristics of low temperature hybrid micro-channel/micro-jet impingement cooling module, Int. J. Heat Mass Transfer 51 (2008) 3882–3895.
[259] M.K. Sung, I. Mudawar, Effects of jet pattern on single-phase cooling performance of hybrid micro-channel/micro-circular-jet-impingement thermal management scheme, Int. J. Heat Mass Transfer 51 (2008) 4614–4627.
[260] M.K. Sung, I. Mudawar, Single-phase and two-phase hybrid cooling schemes for high-heat-flux thermal management of defense electronics, J. Electron. Packag. 131 (2009) 021013.

[261] F. Yang, X. Dai, C.-J. Kuo, Y. Peles, J. Khan, C. Li, Enhanced flow boiling in microchannels by self-sustained high frequency two-phase oscillations, Int. J. Heat Mass Transfer 58 (2013) 402–412.
[262] F. Yang, X. Dai, C. Li, High frequency microbubble-switched oscillations modulated by microfluidic transistors, Appl. Phys. Lett. 101 (2012) 073509.
[263] W. Li, T. Alam, F. Yang, X. Qu, B. Peng, J. Khan, C. Li, Enhanced flow boiling in microchannels using auxiliary channels and multiple micronozzles (II): enhanced CHF and reduced pressure drop, Int. J. Heat Mass Transfer 115 (2017) 264–272.
[264] W. Li, F. Yang, T. Alam, X. Qu, B. Peng, J. Khan, C. Li, Enhanced flow boiling in microchannels using auxiliary channels and multiple micronozzles (I): characterizations of flow boiling heat transfer, Int. J. Heat Mass Transfer 116 (2018) 208–217.
[265] W. Li, X. Qu, T. Alam, F. Yang, W. Chang, J. Khan, C. Li, Enhanced flow boiling in microchannels through integrating multiple micro-nozzles and reentry microcavities, Appl. Phys. Lett. 110 (2017) 014104.
[266] W. Li, J. Ma, T. Alam, F. Yang, J. Khan, C. Li, Flow boiling of HFE-7100 in silicon microchannels integrated with multiple micro-nozzles and reentry microcavities, Int. J. Heat Mass Transfer 123 (2018) 354–366.
[267] X. Dai, F. Yang, R. Fang, T. Yemame, J.A. Khan, C. Li, Enhanced single- and two-phase transport phenomena using flow separation in a microgap with copper woven mesh coatings, Appl. Therm. Eng. 54 (2013) 281–288.
[268] A.K. Vutha, S.R. Rao, F. Houshmand, Y. Peles, Active control of flow boiling oscillation amplitude and frequency using a transverse jet in crossflow, Appl. Phys. Lett. 108 (2016) 134104.
[269] D.D. Meng, J. Kim, C.-J. Kim, A degassing plate with hydrophobic bubble capture and distributed venting for microfluidic devices, J. Micromech. Microeng. 16 (2006) 419–424.
[270] D.D. Meng, T. Cubaud, C.-M. Ho, C.-J. Kim, A methanol-tolerant gas-venting microchannel for a microdirect methanol fuel cell, J. Microelectromech. Syst. 16 (2007) 1403–1410.
[271] M.P. David, J.E. Steinbrenner, J. Miler, K.E. Goodson, Adiabatic and diabatic two-phase venting flow in a microchannel, Int. J. Multiphase Flow 37 (2011) 1135–1146.
[272] M.P. David, J. Miler, J.E. Steinbrenner, Y. Yang, M. Touzelbaev, K.E. Goodson, Hydraulic and thermal characteristics of a vapor venting two-phase microchannel heat exchanger, Int. J. Heat Mass Transfer 54 (2011) 5504–5516.
[273] C. Fang, M. David, A. Rogacs, K. Goodson, Volume of fluid simulation of boiling two-phase flow in a vapor-venting microchannel, Front. Heat Mass Transfer 1 (2010) 013002.
[274] J. Xu, G. Liu, W. Zhang, Q. Li, B. Wang, Seed bubbles stabilize flow and heat transfer in parallel microchannels, Int. J. Multiphase Flow 35 (2009) 773–790.
[275] G. Liu, J. Xu, Y. Yang, W. Zhang, Active control of flow and heat transfer in silicon microchannels, J. Micromech. Microeng. 20 (2010) 045006.
[276] R.R. Bhide, S.G. Singh, A. Sridharan, A. Agrawal, An active control strategy for reduction of pressure instabilities during flow boiling in a microchannel, J. Micromech. Microeng. 21 (2011) 035021.
[277] Y. Han, N. Shikazono, Stabilization of flow boiling in a micro tube with air injection, Exp. Therm. Fluid Sci. 35 (2011) 1255–1264.
[278] Y. Liu, D.F. Fletcher, B.S. Haynes, On the importance of upstream compressibility in microchannel boiling heat transfer, Int. J. Heat Mass Transfer 58 (2013) 503–512.
[279] T.Y. Liu, P.L. Li, C.W. Liu, C. Gau, Boiling flow characteristics in microchannels with very hydrophobic surface to super-hydrophilic surface, Int. J. Heat Mass Transfer 54 (2011) 126–134.
[280] J. Xu, X. Yu, W. Jin, Porous-wall microchannels generate high frequency "eye-blinking" interface oscillation, yielding ultra-stable wall temperatures, Int. J. Heat Mass Transfer 101 (2016) 341–353.
[281] C.J. Kuo, Y. Peles, Flow boiling instabilities in microchannels and means for mitigation by reentrant cavities, J. Heat Transfer 130 (2008) 072402.
[282] C.J. Kuo, Y. Peles, Pressure effects on flow boiling instabilities in parallel microchannels, Int. J. Heat Mass Transfer 52 (2009) 271–280.
[283] S.-M. Kim, I. Mudawar, Review of databases and predictive methods for pressure drop in adiabatic, condensing and boiling mini/micro-channel flows, Int. J. Heat Mass Transfer 77 (2014) 74–97.
[284] S.-M. Kim, I. Mudawar, Universal approach to predicting saturated flow boiling heat transfer in mini/micro-channels – Part I. Dryout incipience quality, Int. J. Heat Mass Transfer 64 (2013) 1226–1238.
[285] C.R. Kharangate, I. Mudawar, Review of computational studies on boiling and condensation, Int. J. Heat Mass Transfer 108 (2017) 1164–1196.